Geophys. J. R. astr. Soc. (1983) 73, 389–426

Synthetic body wave seismograms for laterally varying layered structures by the Gaussian beam method

V. Červený *Institute of Geophysics, Charles University, Ke Karlovu 3, 121 16 Praha 2, Czechoslovakia*

Received 1982 October 20

Summary. Several approaches to computing body wave seismograms in 2-D and 3-D laterally inhomogeneous layered structures are suggested. They are based on the Gaussian beam method, which has been recently applied to the evaluation of time-harmonic high-frequency wavefields in inhomogeneous media. Three variants are discussed in some detail: the spectral method, the convolutory method and the wave-packet method. The most promising seems to be the wave-packet approach. In this approach, the wavefield, generated by a source, is expanded into a system of wave packets, which propagate along rays from the source in all directions. The wave packets change their properties due to diffusion, spreading, reflections/transmissions, etc. The resulting seismogram at any point of the medium is then obtained as a superposition of those packets which propagate close to the point. The final expressions in all the three methods are regular even in regions, in which the ray method fails, e.g. in the vicinity of caustics, in the critical region, at boundaries between shadow and illuminated regions, etc. Moreover, they are not as sensitive to the minor details of the medium as the ray method and, what is more, they remove the time-consuming two-point ray tracing from computations. Numerical examples of synthetic seismograms computed by the wave-packet approach are presented.

1 Introduction

Various alternative methods are now available for evaluating body wave synthetic seismograms in vertically inhomogeneous and radially symmetric media. The situation is, however, more complicated in 2-D and 3-D laterally inhomogeneous media with curved interfaces. For these types of media, analytical solutions of the elastodynamic equation are not known. The three most common approaches to the investigation of seismic wavefields in such complex 2-D and 3-D structures are: (a) methods based on direct numerical solutions of the elastodynamic equation, such as the finite-difference and the finite-element method: (b) the perturbation method; (c) the approximate high-frequency asymptotic methods. We do not intend to give a review of all these methods here, because it can be found elsewhere (see, e.g. Richards 1979; Aki & Richards 1980; Chapman & Drummond 1983; Červený *et al.* 1981).

Here, we shall pay attention only to high-frequency approximate methods, which are most suitable for investigating seismic body waves in models which are large in comparison with the prevailing wavelength, e.g. in the Earth's crust and the uppermost mantle.

A typical high-frequency approximate method is the ray method. The ray method has found many useful applications in seismology (see Červený, Molotkov & Pšenčík 1977; Aki & Richards 1980). Effective programs to evaluate the ray synthetic seismograms exist both for 2-D and 3-D laterally inhomogeneous, layered structures. For more details and examples of computations of ray synthetic seismograms in 2-D media refer to, e.g. Hron & Kanasewich (1971), Červený *et al.* (1977), Červený & Pšenčík (1977), Hron, Daley & Marks (1977), Hong & Helmberger (1977), May & Hron (1978), Červený (1979), McMechan & Mooney (1980), Červený & Pšenčík (1981) and Cassell (1982). Similarly, for 3-D media see Klimeš (1982a) and Červený, Klimeš & Pšenčík (1982).

The ray method, however, has certain disadvantages. In principle, it can only be applied to smooth media, in which the characteristic dimensions of all inhomogeneities are considerably larger than the prevailing wavelength of the propagating wave. Even in the case of smooth media, the ray method has some other limitations. We shall mention two of them here. *The first major problem* consists in its limited accuracy in the so-called singular regions (caustic region, critical region, transition between shadow and illuminated region, etc.). Unfortunately, particularly the singular regions are often very important in the interpretation, as the amplitudes of body waves reach their maximum values there. Various modifications of the ray method have been suggested which increase considerably the accuracy of ray methods in singular regions. However, they are of limited value, because they can only be applied to simple separated singular regions, and singular regions in laterally inhomogeneous layered structures very often overlap. Moreover, the modifications complicate considerably the algorithms for evaluating synthetic seismograms. *The second problem* is connected with the high sensitivity of ray amplitudes to the approximation of the medium and to the thin details of the model (such as the artificial interfaces of higher order and edges in interfaces, small fictitious oscillations of the velocity function introduced by approximation methods, etc.). Very often, these small details are responsible for the anomalous behaviour of ray amplitude–distance curves and ray synthetic seismograms.

There is yet another difficulty in evaluating ray synthetic seismograms which is not principal from a physical point of view, but which complicates the computer algorithms and computations. It is connected with the necessity to perform two-point ray tracing. It makes the evaluation of synthetic seismograms rather cumbersome and time consuming, particularly in 3-D media.

An extensive literature is devoted to the problem of high-frequency asymptotics for the seismic wavefield in individual singular regions. Several asymptotic high-frequency approaches, however, treat the problem of singularities from a more general point of view. Let us mention some of them.

One of these methods is the well-known *parabolic equation method.* The method was first used by Leontovich and Fock in investigating the propagation of electromagnetic waves around the Earth (Leontovich & Fock 1946; Fock 1965). Since then the method has been used in many wave-propagation applications, in which the waves propagating in certain preferred direction were studied (Babich & Buldyrev 1972; Landers & Claerbout 1972; Babich & Kirpichnikova 1974; Claerbout 1976; McCoy 1977; Tappert 1977; Hudson 1980, etc.). The method has also been applied to study of solutions concentrated close to rays (Gaussian beams), as will be discussed in detail later.

Another promising method is based on the applications of *Kirchoff's integral* (Hilterman 1970, 1975; Trorey 1970, 1977; Haddon & Buchen 1981; Buchen & Haddon 1981; Sinton

& Frazer 1981, etc.) Klem-Musatov (1980) proposed a modification of the seismic ray method for piecewise block structures, based on the application of *edge waves*. Similarly, a new general approach to the evaluation of finite frequency body wave seismograms in laterally inhomogeneous media, based on the generalization of the *phase integral method*, was suggested by Frazer & Phinney (1980) and Sinton & Frazer (1982). A rigorous, but simple method for evaluating synthetic body wave seismograms, based on the application of *Maslov's asymptotic theory* (Maslov 1965, 1977) was proposed by Chapman & Drummond (1983). The method is quite general; it avoids the oscillatory integrals of the asymptotic theory and provides smoothed, discrete seismograms directly.

An alternative general method for the evaluation of time-harmonic wavefields in 2-D and 3-D structures was suggested recently. It is based on the simulation of the high-frequency wavefield by a system of *Gaussian beams,* concentrated close to rays (see extensive references in Sections 2 and 3). The wavefield concentrated close to rays is evaluated by the parabolic equation method. Solutions of the parabolic wave equation (Schrödinger equation) decrease exponentially with the increasing square of distance from the ray. Thus, the amplitude profile perpendicular to the ray is bell-shaped. This is the reason why these solutions are called Gaussian beams. The width and curvature of the phase front of the beam change along the ray due to diffusion, to spreading and reflections/transmissions as the wave progresses. The final expressions for the Gaussian beams are regular even at caustics. More details on Gaussian beams will be given in Section 2.

The time-harmonic wavefield generated by a specified source is then evaluated as follows: the wavefield in the neighbourhood of the source is expanded into a system of Gaussian beams. Each beam is continued along the corresponding ray and the final wavefield at any point is obtained as a superposition of all the beams arriving in some neighbourhood of the receiver. The asymptotic expansions into Gaussian beams are still only known for simple types of sources, but we believe that similar expansions will be soon found even for more realistic types of sources. For details on these expansions see Section 3.

The method of Gaussian beams effectively combines the broad possibilities of the ray method and the accuracy of wave methods. For numerical examples of computing time-harmonic seismic wavefields by the Gaussian beam approach in various singular regions refer to Katchalov & Popov (1981) for a wavelength, to Červený, Popov & Pšenčík (1982a) for caustic region, and to Hronová (1982) for critical regions.

In this paper, we are primarily interested in evaluating synthetic seismograms, not in the time-harmonic wavefield. Several approaches can be used to change the Gaussian beam approach, described above, from the frequency domain to the time domain.

It is simplest to apply the Fourier transform (see Section 4.1). The expressions it yields give an approximate high-frequency generalization of the well-known reflectivity method (see Fuchs 1968; Fuchs & Müller 1971) for laterally inhomogeneous 2-D and 3-D layered structures. The other possibility is to rewrite the obtained solution in terms of convolutory integrals. In this approach, the oscillatory integrals of the spectral method are replaced by simple, non-oscillatory integrals which resemble, in many respects, the slowness method suggested by Chapman (1978) and the Wiggins disc ray theory (see Wiggins 1976). Our integrals are, however, applicable to laterally inhomogeneous 2-D and 3-D structures (for details see Section 4.2). The third possibility consists in the application of the Fourier transform or convolution directly to individual Gaussian beams. In this way, the wave packets which propagate along rays are obtained. The final expressions for the wave packets are surprisingly simple. The synthetic seismogram at any point of medium is obtained by a superposition of all wave packets which propagate in the neighbourhood of the point.

A special case of wave packets are delta packets and Gaussian packets. The Gaussian

packets have approximately a bell-shaped envelope both in time and space. The expressions for the delta packets and Gaussian wave packets can be written analytically. This makes the evaluation of synthetic seismograms very effective and fast.

The Gaussian beam approach removes the two main problems of the ray method, listed above. The final expressions for synthetic seismograms are regular even in regions where the ray fields are singular no matter how complicated the singular regions are (they may, of course, overlap). Similarly the final expressions are not so sensitive to the details in the structure of the medium as the ray method. The smoothing effect is, of course, frequency dependent. With increasing prevailing frequency, also the resolving power of the method increases. Finally, two-point ray tracing is not needed in the method; the ray field may be computed by initial-value ray tracing. This is a very useful property, particularly in computing synthetic seismograms in 3-D media (see Klimeš 1982b).

Note that the Gaussian beam approach can be formally used even in the limiting case of infinitely broad Gaussian beams. In this case, the expressions for the Gaussian beam give the *paraxial ray approximation.* The integral superposition of Gaussian beams leads to the superposition of paraxial approximations, constructed along individual rays. At any point of the medium, the wavefield can be obtained as a superposition of the paraxial ray approximations corresponding to rays passing in the close neighbourhood of the receiver; the paraxial ray approximations corresponding to remote rays do not contribute to the final wavefield due to *destructive interference.*

The algorithms and programs for evaluating body wave seismograms, based on the Gaussian beam approach, are no more complicated than those based on the standard ray method. They may even be simpler. The reason for this is that two-point ray tracing is not needed in these programs. The computation itself may also be faster than the evaluation of ray synthetic seismograms, mainly if the synthetic seismograms have to be computed at many receiver positions. As soon as a sufficiently dense system of rays is determined, the evaluation of synthetic seismograms at any point situated in the region covered by the system of rays is fast and easy.

For completeness, note that two-point ray tracing can be avoided even in the evaluation of *ray* synthetic seismograms; it may be replaced by dynamic ray tracing and the paraxial ray approximation. This approach is very useful particularly in 3-D media and for sources situated outside the profile. For details refer to Klimeš (1982a) and to Červený *et al.* (1982).

Any program for ray tracing and ray amplitude computation in 2-D and 3-D media, in which geometrical spreading is computed by dynamic ray tracing, can be easily adapted to the Gaussian beam approach. The program package SEIS81 (Červený & Pšenčík 1981) for evaluating ray synthetic seismograms in 2-D laterally inhomogeneous structures was rewritten in this way for the Gaussian packet computations. The program was tested on various simple structures (see details in Section 5). All the results are promising. A similar program was written for 3-D laterally inhomogeneous layered structures by Klimeš (1982b). Numerical tests show that the Gaussian packet approach is effective even in 3-D media. It is, of course, more time-consuming, as a two-parametric system of rays must be computed.

2 Gaussian beams

Let us consider a scalar wave equation or a vectorial elastodynamic equation, and the corresponding wavefield. Let us select an arbitrary ray and denote it by Ω. In case of the elastodynamic equation, this may be the ray of either a compressional (P) or a shear (S) wave. We introduce the ray-centred coordinate system (s, q_1, q_2) connected with this ray. The coordinate s measures the arc length along the ray Ω from an arbitrary reference point, q_1

and q_2 represent the length coordinates perpendicular to the ray at s. The vector basis of the new coordinate system is formed by the triplet of unit vectors $\mathbf{t}$, $\mathbf{e}_1$, $\mathbf{e}_2$, where $\mathbf{t}$ is tangent to Ω and $\mathbf{e}_1$, $\mathbf{e}_2$ are perpendicular to Ω. They are specified in such a way that the coordinate system (s, q_1, q_2) is orthogonal. In other words, (s, q_1, q_2) form a natural coordinate system connected with the ray Ω. This ray-centred coordinate system was introduced into seismology by Popov & Pšenčík (1978a, b) (for details see also Červený & Hron 1980). Note that the ray-centred coordinate system (s, q_1, q_2) is not regular at larger distances from the ray Ω when the ray Ω is curved. We consider here only a region along Ω at which the ray-centred coordinate system (s, q_1, q_2) is regular and call it 'the regularity region'.

The ray-centred coordinate system is suitable for studying the high-frequency part of the wavefield which propagates along the ray Ω. It is not difficult to show that the high-frequency solutions of the wave equation and of the elastodynamic equation, concentrated close to the ray Ω, can be expressed in terms of the solutions of the parabolic equation. From a physical point of view, these solutions represent Gaussian beams, their amplitude profiles perpendicular to the central ray Ω are bell-shaped (Gaussian). In the limiting case of an infinitely broad Gaussian beam, they represent the paraxial ray approximation. (We consider these solutions, of course, only in the regularity region along Ω, even when we formally speak about the infinitely broad Gaussian beams.)

The parabolic equation method was first used to study the solutions of a wave equation, concentrated close to a ray, by Babich (1968). The asymptotic analytical expressions for Gaussian beams, concentrated close to rays, are now known both for the wave equation and for the elastodynamic equation, even for general multiply reflected and refracted rays in layered inhomogeneous media. For references see Kirpichnikova (1971), Babich & Buldyrev (1972), Babich & Kirpichnikova (1974), Babich & Popov (1981), Popov (1981, 1982), Červený (1981a, 1982), Červený *et al.* (1982a), Červený & Pšenčík (1983) and Klimeš (1982b). Similar expressions for Gaussian beams can undoubtedly be easily written even for other types of wavefields in laterally inhomogeneous layered structures.

All the above-mentioned solutions refer to the frequency domain. To adjust the time-harmonic Gaussian beams to the time domain, it is not necessary to present detailed formulae for the time-harmonic Gaussian beams. It is sufficient to write these expressions in some schematic form, which remains valid in all situations (even in situations for which the concrete formulae for Gaussian beams have not yet been derived). We shall give all the expressions for a 3-D case; the specification for a 2-D case is straightforward.

We consider a time-harmonic Gaussian beam with the circular frequency ω. We assume that the frequency ω is positive and high. The factor $\exp(-i\omega t)$, where t is the time, is omitted in the following equations. We denote by $V(s, q_1, q_2)$ the velocity of propagation. In case of elastodynamic Gaussian beams, $V(s, q_1, q_2)$ may be the velocity of either a compressional wave (when the Gaussian beam is concentrated close to the ray of the P-wave) or a shear wave (for the Gaussian beam concentrated close to the ray of the S-wave). We shall also use the notation $v(s) = V(s, 0, 0)$. In this way, $v(s)$ denotes the velocity measured at the central ray Ω.

Let us now consider a point S, situated close to the ray Ω, specified by the ray-centred coordinates (s, q_1, q_2), i.e. $S \equiv [s, q_1, q_2]$. The scalar Gaussian beam, connected with the central ray Ω, then gives the following contribution at point S,

$$u(S, \omega) = A(s) \exp \{i\omega\theta(s, q_1, q_2) - \omega G(s, q_1, q_2)\}. \tag{1}$$

Here $u(S, \omega)$ may represent various physical quantities in various wave propagation problems. The same equation can be used even for the vectorial solution, only the scalar quantities $u(S, \omega)$ and $A(s)$ must be replaced by vectorial quantities $\mathbf{u}(S, \omega)$ and $\mathbf{A}(s)$.

For simplicity, only the scalar solutions will be given in the following, which can be simply changed to vectorial solutions in any case under consideration. By the argument S we understand three variables – the coordinates of the point S.

The quantity $A(s)$ in (1) is a complex-valued amplitude factor which does not depend on ω and on the coordinates q_1, q_2. For Gaussian beams with a finite width, $A(s)$ remains finite along the whole ray Ω; *it has no singularity at the caustic.* It has exactly the same form as the corresponding amplitude factor in the ray method (see Červený *et al.* 1977; Pšenčík 1979), only the geometrical spreading is replaced by a complex-valued function which does not vanish at any point of the ray. We shall call this function *the complex-valued spreading.* (Remember that geometrical spreading in the ray method is either real or imaginary.) More details on the complex-valued spreading will be given later. In case of a multiply reflected/refracted ray, the quantity $A(s)$ also contains the product of reflection/transmission coefficients at the individual points of incidence at interfaces, the coefficient of conversion, etc. In case of elastodynamic Gaussian beams, the scalar quantity $A(s)$ should be replaced by the vectorial quantity $\mathbf{A}(s)$. (For simplicity, we consider here only the principal components of the elastodynamic Gaussian beam.) For Gaussian beams concentrated close to the ray Ω of a P-wave, $\mathbf{A}(s)$ points along the ray Ω. The situation is more complicated for a Gaussian beam concentrated close to the ray of an S-wave, when $\mathbf{A}(s)$ is perpendicular to the ray Ω. In an inhomogeneous medium without interfaces, the components of $\mathbf{A}(s)$ into $\mathbf{e}_1$ and $\mathbf{e}_2$ are not coupled to each other and propagate independently, even when the ray Ω is three-dimensional with non-zero torsion. Both the components, however, may become coupled when the ray strikes an interface.

The phase factor $\theta(s, q_1, q_2)$ again does not depend on the frequency ω, but it depends on all the three ray-centred coordinates of the point S, namely s, q_1, q_2. It is given by the relation

$$\theta(s, q_1, q_2) = \tau(s) + \frac{1}{2v(s)}\, q^{\mathrm{T}} \mathsf{K}(s)\, q, \tag{2}$$

where

$$\tau(s) = \tau(s_0) + \int_{s_0}^{s} v^{-1}(\zeta)\, d\zeta, \quad q = \begin{pmatrix} q_1 \\ q_2 \end{pmatrix}, \quad q^{\mathrm{T}} = (q_1, q_2). \tag{3}$$

The integral in (3) is taken along Ω and ζ denotes the arc-length along Ω. The symbol T denotes the transpose. Finally $\mathsf{K}(s)$ is a 2×2 symmetrical real-valued matrix, not specified here. It can be interpreted as the *curvature matrix of the phase front of the Gaussian beam.* The first term in (2), $\tau(s)$, measures the travel time along the ray Ω.

The expression $G(s, q_1, q_2)$ in equation (1) controls the decay of amplitudes of the Gaussian beam in the direction perpendicular to the ray Ω and can be expressed as

$$G(s, q_1, q_2) = \tfrac{1}{2} q^{\mathrm{T}} \mathsf{B}(s)\, q, \tag{4}$$

where $\mathsf{B}(s)$ is a 2×2 positive definite real-valued matrix, q and q^{T} being given by (3).

Note that a complex-valued 2×2 matrix $\mathsf{M}(s)$, given by the expression

$$\mathsf{M}(s) = \frac{1}{v(s)}\, \mathsf{K}(s) + i\mathsf{B}(s), \tag{5}$$

(where i is the imaginary unit) may be introduced. The quantity $\mathsf{M}(s)$ may then be called the complex-valued *matrix of second derivatives of the travel-time field* and $v(s)\, \mathsf{M}(s)$ the complex-valued *curvature matrix.* Using $\mathsf{M}(s)$, equation (1) for the Gaussian beam can be

written as follows:

$$u(s, \omega) = A(s) \exp \{i\omega [\tau(s) + \tfrac{1}{2} q^{\mathrm{T}} \mathsf{M}(s) q]\} . \tag{6}$$

Matrix $\mathsf{M}(s)$ is a complex-valued solution of the matrix Riccati equation,

$$\frac{d\mathsf{M}}{ds} + v\mathsf{M}^2 + v^{-2}\mathsf{V} = 0, \tag{7}$$

where $\mathsf{V}(s)$ is a real-valued 2×2 matrix with elements V_{ij} given by the expression

$$V_{ij} = [\partial^2 V(s, q_1, q_2)/\partial q_i \partial q_j]_{q_1 = q_2 = 0}.$$

The non-linear Riccati equation (7) can be rewritten into a system of two matrix linear ordinary differential equations of the first order introducing new 2×2 complex-valued matrices Q and P by the relations $\mathsf{M} = v^{-1} d\mathsf{Q}/ds\, \mathsf{Q}^{-1} = \mathsf{P}\mathsf{Q}^{-1}$. The system reads

$$\frac{d\mathsf{Q}}{ds} = v\mathsf{P}, \quad \frac{d\mathsf{P}}{ds} = -v^{-2}\mathsf{V}\mathsf{Q}. \tag{8}$$

Note that the complex-valued spreading discussed above is given by the expression $(\det \mathsf{Q})^{1/2}$.

In a 2-D case, all the above equations remain valid, only the 2×2 matrices (K, B, M, V, Q, P) are replaced by scalars (K, B, M, V, Q, P), corresponding, e.g. to the upper left elements of corresponding matrices. The vector q from (3) is also replaced by its first component.

The real-valued form of the above differential equations has found broad applications in the ray method. The systems (7) and (8) are called in this case the *dynamic ray tracing systems,* and the matrix B and the quantity G identically vanish. Equation (1) can be used effectively even in this case. It describes the wavefield in the close neighbourhood of the specified ray Ω. We shall call it here the *paraxial ray approximation.* In this sense, the paraxial ray approximation corresponds formally to an infinitely broad Gaussian beam. The curvature matrix of the phase front of the beam $\mathsf{K}(s)$ yields then the standard curvature matrix of the wavefront, and the complex-valued spreading $(\det \mathsf{Q})^{1/2}$ reduces to the geometrical spreading of the standard ray theory. The paraxial ray approximation is, of course, singular at caustics, where the geometrical spreading vanishes. For references see Popov (1977), Popov & Pšenčík (1978a, b), Červený & Hron (1980), Hubral (1979, 1980), Azbel, Dmitrieva & Yanovskaya (1980) and Červený (1981a, c). A detailed discussion of various applications of the dynamic ray tracing in 2-D media in seismology and in seismic prospecting can be found in Červený (1981c). The dynamic ray tracing can be used to evaluate the second derivatives of the travel-time field, the curvatures of the wavefront, the geometrical spreading, etc. It can also be applied to perform a simple and fast ray tracing in the vicinity of a known specified central ray Ω (including the two-point ray tracing). Several applications in seismic prospecting are described in Gol'din (1979) and in Hubral & Krey (1980).

The complex-valued form of the dynamic ray tracing systems (7) and (8) was discussed by Babich (1968), Kirpichnikova (1971), Babich & Buldyrev (1972), Popov (1981) and Červený (1981a, 1982). For a 2-D version of the complex-valued systems see Babich & Kirpichnikova (1974), Červený (1981a), Červený *et al.* (1982a) and Červený & Pšenčík (1983). It should be noted that any complex-valued solution of (8) can be constructed from a system of real-valued linearly independent solutions of (8). The complex-valued solution is obtained as a superposition of the real-valued linearly independent solutions, multiplied by some complex-valued constants. These constants fully determine the behaviour of the Gaussian beam along the whole ray Ω (i.e. both the curvature matrix of the phase front of

the Gaussian beam $\mathsf{K}(s)$ and the matrix $\mathsf{B}(s)$, controlling the amplitude profiles perpendicular to Ω). We shall call these constants the *initial parameters of Gaussian beams.* It was shown by Červený *et al.* (1982a), that the Gaussian beam in a 2-D medium is fully specified by two real-valued initial parameters, e.g. by the curvature of the phase front and the half-width of the beam at $s = s_0$. The 3-D Gaussian beam is specified by six real-valued initial parameters. Simpler types of 3-D Gaussian beams can be specified by a lower number of initial parameters. For example, a 3-D *circular* Gaussian beam is fully specified by only two real-valued initial parameters. A more detailed discussion of this problem will be published elsewhere.

As we have seen above, the evaluation of Gaussian beans is algorithmically very similar to the evaluation of ray solutions. In fact, the algorithms for the evaluation of Gaussian beams may be even simpler than these for the ray solutions. No special attention must be devoted to the caustic point in the evaluation of Gaussian beams, the caustic points are quite standard and regular points in this case. In the ray theory, however, a familiar phase retardation of $\frac{1}{2}\pi$ or π must be introduced at each point where the ray trajectory touches the caustic surface. Thus, a permanent attention must be devoted to the position of caustic points and to the type of the caustic when evaluating the ray solutions. Of course, the same applies to the paraxial ray approximations.

Equation (1) is not the only solution of the parabolic equation. When $G \neq 0$, an infinite number of linearly independent solutions of the parabolic equation can be constructed using Hermite polynomials; the solution (1) being the basic (zero) mode. In the following, we shall consider only the basic mode (1). (The higher modes can find applications, e.g. in various problems of diffraction of Gaussian beams and of constructing beams with a non-Gaussian amplitude profile.)

Similarly, we shall not discuss the higher terms of the asymptotic series for $U(S, \omega)$ in powers of $1/(-i\omega)^{1/2}$ here. For example, in the case of elastodynamic Gaussian beams, the Gaussian beam concentrated close to the ray of a *P*-wave also has transverse components, perpendicular to the ray. Similarly, the Gaussian beam concentrated close to the ray of an *S*-wave also has a longitudinal component, parallel to the ray. These 'additional components', however, are of a higher order than the principal components and will not be discussed here. For details see Kirpichnikova (1971), Červený & Pšenčík (1983) and Klimeš (1982b).

As mentioned above, the complex-valued amplitude factor $A(s)$ in (1) does not depend on frequency. Similarly as in the ray method, it may be useful to modify our results slightly and allow some factors in $A(s)$ to be frequency-dependent. One such a situation is described in the following. Let us consider the model of a medium, composed of thick inhomogeneous layers separated by thin transition layers with abrupt changes of velocity. A modification of the ray method was suggested by Ratnikova (1973) for vertically inhomogeneous layered structures, in which the ray theory is applied to thick vertically inhomogeneous layers and the reflection/transmission coefficients at transition layers are evaluated by matrix methods, e.g. by the Thompson-Haskel method. Then the reflection/transmission coefficients are frequency-dependent and the quantity $A(s)$ also becomes frequency-dependent. The hybrid ray-matrix method described above has been used broadly in various applications. See also a short description of the method in Červený *et al.* (1977). Daley & Hron (1982) used an analogous method to study the *SH*-waves in stacks of thin and thick layers and called it the ray-reflectivity method. In the Gaussian beam approach, this modification is even more natural than in the ray method (see more details in Section 4).

In the conclusion of this section it should be emphasized that our attention has been devoted to the high-frequency Gaussian beams, concentrated close to a ray Ω in an inhomogeneous medium. We found that these Gaussian beams are the solutions of the parabolic

equation. Gaussian beams, however, can be derived and investigated also by other approaches, particularly in some special situations (e.g. in a piecewise homogeneous medium). They have found many important practical applications in optics, electromagnetic waves, acoustics, and even in seismic prospecting. For references see Kogelnik (1965), Deschamps (1971), Marcuse (1972), Felsen & Marcuvitz (1973), Felsen (1976) and Claerbout (1981a, b).

3 Expansion of the wavefield into Gaussian beams

Let us now consider a wavefield (scalar or vectorial) generated by some idealized source. Examples are a point source, a line source, a 'plane' source, etc. The source may, generally, be more complex, we only assume that the corresponding system of rays is two-parametric and that it uniquely determines the system of wavefronts (orthonomic system of rays, see Stavroudis 1972). We denote the two ray parameters by ϕ, δ. They may have a different meaning in different wave-propagation problems. They may correspond to some angles or direction cosines or slowness vector components in some problems, and may have the dimension of length in other problems. For example, in the case of a point source, ϕ and δ may be taken as the take-off angles at the point source. They specify the initial direction of the ray at the source. In the case of a line source, ϕ may be the polar angle in the plane perpendicular to the line source and δ the length along the source, measured from some reference point at the line source. The ray parameters can also be specified along a selected wavefront of the wave; they may be regarded as curvilinear coordinates on the wavefront. In case of a plane wave, ϕ and δ may be the Cartesian coordinates in the plane. In case of a more complex source, ϕ and δ may be specified in a similar way.

The Gaussian beam procedure can even be applied to more complex sources, for which the wavefield can hardly be described by an orthonomic system of rays. In such cases, it would be possible to use the principle of superposition and form the source by superimposing simpler sources, for which the assumption is valid. The whole procedure will, of course, be simpler if we consider sources for which the ray field forms an orthonomic two-parameter system of rays.

We shall discuss a general 3-D case here. For a 2-D problem, the orthonomic system of rays will, naturally, be one-parametric.

Babich & Pankratova (1973) first suggested describing the wavefield in the high-frequency approximation by means of an expansion into the solutions concentrated close to the rays. According to Babich & Pankratova (1973), such a proposal was made even earlier by V. S. Buldyrev and V. F. Lazutkin at a seminar on diffraction and wave propagation of LOMI (Mathematical Institute of the Academy of Sciences of the USSR, Leningrad Division). Such asymptotic expansions are now known for several types of sources, both for the wave equation and for the elastodynamic equation. For a point source, refer to the details in Popov (1981, 1982) and Klimeš (1982b), for a line source to Červený *et al.* (1982a). For a plane wave, the expansion of the plane wave into Gaussian beams is exact, valid even for small ω (Červený 1981a, 1982). A summary of various expansions can be found in Červený (1981a). It will not be complicated to write such expansions for even more complex types of sources.

As in the case of Gaussian beams, we shall write the equations for the asymptotic high-frequency expansions of the wavefield into Gaussian beams only in a schematic form, which remains valid in various situations (hopefully even in situations for which the concrete form of these expansions has not yet been derived). To distinguish between the wavefield corresponding to an individual Gaussian beam (1) and the wavefield obtained by super-

position of Gaussian beams, we shall use, in the latter case, the capital U, instead of the lower-case u, reserved for individual Gaussian beams. Note that the wavefield $u(S, \omega)$ corresponding to an individual Gaussian beam (given by 1) is a function of ray parameters ϕ, δ, which specify its central ray Ω under consideration. Thus, we shall write $u(S, \omega, \phi, \delta)$ instead of $u(S, \omega)$.

Let us assume that the medium in the vicinity of the source is locally homogeneous and again denote the observation point by S. We can then express the wavefield $U(S, \omega)$ as

$$U(S, \omega) = (-i\omega)^{k/2} \int_{\phi_0}^{\phi_N} \int_{\delta_0}^{\delta_M} \Phi(\phi, \delta)\, u(S, \omega, \phi, \delta)\, d\phi\, d\delta. \tag{9}$$

$\Phi(\phi, \delta)$ is some complex-valued function not specified here, which depends on the type of source. The limits in both integrals, ϕ_0, ϕ_N and δ_0, δ_M, may be different for different sources. They must be chosen in such a way as to guarantee that the Gaussian beams, concentrated close to rays with parameters $\bar{\phi}$, $\bar{\delta}$ outside the range of integration limits, do not contribute effectively to the complete wavefield at S. The factor $(-i\omega)^{k/2}$ is optionally included in the expansion formula (9) to obtain a frequency-independent far-field amplitude of the generated wavefield. In the known expansion formulae mentioned above, the quantity k was found to be different for 2-D and 3-D media. For a 3-D case, with a double integral in (9), the quantity k was found to equal 2. Equation (9), however, can also be applied to a 2-D case [superposition of 2-D Gaussian beams $u(S, \omega, \phi)$]. Then it contains only one integral over ϕ, and k equals 1.

As was shown in Section 2, the expression $u(S, \omega, \phi, \delta)$ for Gaussian beams can be used only in the regularity region along the ray Ω specified by the ray parameters ϕ, δ. Therefore, the function $u(S, \omega, \phi, \delta)$ in the integral (9) should be multiplied by some windowing function which vanishes outisde the regularity region. The influence of the artificially introduced windowing function on the final results will be generally small. Since we usually work with narrow beams, the situation that $u(S, \omega, \phi, \delta)$ is not negligible outside the regularity region will occur only exceptionally. Even in the case of broad Gaussian beams, however, the influence of the windowing function is expected to be small due to the effects of the destructive interference of remote Gaussian beams. (The effect of the destructive interference will be briefly discussed later.)

Note that the coordinates of point S in the expression $U(S, \omega)$ on the lhs of (9) may be specified in any general coordinate system. In the integrand on the rhs of (9), however, S is specified by the ray-centred coordinates (s, q_1, q_2) corresponding to individual rays with parameters ϕ and δ. In other words, the quantities s, q_1, q_2 depend on ϕ and δ.

Equation (9) can again be written even for a vectorial case (e.g. for elastic waves). The scalar quantities $U(S, \omega)$ and $u(S, \omega, \phi, \delta)$ in (9) should then be replaced by vector quantities $\mathbf{U}(S, \omega)$ and $\mathbf{u}(S, \omega, \phi, \delta)$.

When the integrand of (9) is sufficiently smooth for given S and ω, the integral (9) may be evaluated by numerical quadratures. This gives

$$U(S, \omega) = (-i\omega)^{k/2} \sum_{i=0}^{N} \sum_{j=0}^{M} \Phi(\phi_i, \delta_j)\, u(S, \omega, \phi_i, \delta_j)\, \Delta\phi_i\, \Delta\delta_j, \tag{10}$$

where the quantities $\Delta\phi_i$ and $\Delta\delta_j$ are determined from a given system of ϕ_i and δ_j ($i = 0, 1, 2, \ldots, N$; $j = 0, 1, \ldots, M$) in agreement with specific numerical quadrature procedure. Note that equation (9) gives a continuous and equation (10) a discrete expansion of the wavefield into Gaussian beams.

In the case of a layered medium, a large number of various multiply reflected/refracted,

possibly converted, waves may propagate in the medium. The expansion (9) or (10) must then be written for each of these waves and the complete wavefield is obtained as the superposition of all these expansions. The situation is fully equivalent to the ray method in this respect. In stacks of thick and thin layers, the number of waves can be radically decreased if the modification with frequency-dependent reflection/transmission coefficients, described at the end of the preceding section, is applied.

The accuracy of the asymptotic integral (9) or of its discrete version (10) depends on various parameters. The most straightforward way to investigate it is based on numerical computations of test examples. Certain such computations will be presented in Section 5; a more extensive investigation was performed by Hronová (1982) and will be described elsewhere. Some analytical estimates regarding the accuracy of equation (9) for a point source in a 3-D medium were found by Klimeš (1982b).

Let us now summarize the procedure of computing the time-harmonic wavefield generated, say, by a point source. For simplicity, we shall consider only one elementary wave; the procedure may be repeated for all waves under consideration. The procedure is as follows:

First, a sufficiently dense, regular or irregular, system of rays running from a source in various directions, specified by ray parameters ϕ_i, δ_j ($i = 0, 1, 2, \ldots, N$; $j = 0, 1, 2, \ldots, M$) is computed. The rays are computed as an initial-value (Cauchy) problem. The computed rays must cover the whole region in which the receivers are situated, with some reserve of rays outside this region.

Secondly, the dynamic ray tracing system (8) is solved several times to obtain all its linearly independent solutions. (For example, in a 2-D medium, the system (8) has two linearly independent solutions and must be solved twice.)

Thirdly, the ray-centred coordinates of the receiver point S are found for all rays. For each individual ray, the functions $\tau(s)$, $\mathsf{K}(s)$, $\mathsf{B}(s)$ and $A(s)$ (or some other alternative functions) are determined. If we know all these functions, we can compute the Gaussian beam connected with the ray under consideration. The Gaussian beams corresponding to remote rays having no substantial effect on the results at the point S are eliminated, only beams passing in the neighbourhood of the point S need be considered.

Fourthly, the wavefield at the receiver point S is then obtained by a weighted superposition of contributions, corresponding to individual beams (see equation 9 or 10).

The great advantage of the procedure described above in comparison with the ray method is that the rays may be computed as an initial-value (Cauchy) problem and that time-consuming two-point ray tracing is not required. This makes the computer algorithms for evaluating the wavefield, based on the Gaussian beam approach, simpler than the algorithms based on the ray method. For the same reason, the application of the Gaussian beam approach may be even less time-consuming than the applications of the standard ray method.

Moreover, as soon as the region under consideration is covered by rays and these results are stored in the computer, the wavefield can simply be computed at any point of the region. It is not necessary to repeat the ray tracing and the dynamic ray tracing if we are interested in the wavefield in a new system of receivers within the region under investigation.

For more details on the procedure see Babich & Pankratova (1973), Popov, Pšenčík & Červený (1980), Popov (1981, 1982), Katchalov & Popov (1981), Červený (1981a, 1982), Červený *et al.* (1982a), Červený, Popov & Pšenčík (1982b), Hronová (1982) and Klimeš (1982b).

Some difficulties appear in step 3 of the procedure. The determination of the ray-centred coordinates (s, q_1, q_2) of the receiver point S, connected with a ray Ω, is simple (see details

in Červený *et al.* 1982a, section 6). However, it requires that the trajectories of all computed rays, together with a number of auxiliary quantities at all points of these rays, are stored in the computer. A simplified approach based on the paraxial ray approximation can be applied in certain situations which removes this difficulty (see Červený 1981c). For example, when the receiver point is situated close to the Earth's surface, all the necessary parameters of Gaussian beams can be determined from the termination points of the rays along the Earth's surface. In this way, only the termination points of the rays at the Earth's surface (not the whole rays) together with the auxiliary quantities determined at these points can be stored in the computer.

As was shown in Section 2, Gaussian beams remain regular even at caustics and in their neighbourhood where the ray method itself is singular. There may, however, still be some other singularities in the ray field. The integration (9) removes most of these singularities. The singularities of the ray method, which are removed by the integration in (9), are connected, e.g. with the singular behaviour of reflection/transmission coefficients (e.g. critical regions), boundaries of shadow zones, etc. Using (9) or (10), the wavefield penetrating into a half-shadow is automatically obtained. (The wavefield in the deep shadow, however, is not obtained.)

Let us emphasize one interesting point. Integral (9) remains valid even for infinitely broad Gaussian beams $u(S, \omega, \phi, \delta)$, assuming that the windowing function discussed above is used. Integral (9) represents in this case an expansion of the wavefield into the paraxial ray approximations connected with the orthonomic system of rays. It leads easily to various local asymptotics known from the literature. In contrast to these asymptotic results, derived usually for simple, specific situations (e.g. for vertically inhomogeneous media), equation (9) can be used quite generally for 3-D laterally inhomogeneous media with curved interfaces. To evaluate integral (9), the method of stationary phase and its various well-known modifications can be used. The method of stationary phase also shows that only the rays passing close to the receiver S contribute effectively to the wavefield at S. The reason for this is the destructive interference of paraxial ray approximations corresponding to remote rays, not the amplitude decrease of beams perpendicular to the ray.

It would be also possible to interpret these results using the terminology of Fresnel zones and Fresnel volumes known from optics, see Born & Wolf (1968), Kravcov & Orlov (1980, section 10). The energy arriving at the receiver is due not only to the ray propagating with the stationary travel time, but also due to the bundle of neighbouring rays.

4 Construction of synthetic seismograms

In the two preceding sections, we considered the propagation of time-harmonic waves. It is not difficult to rewrite the results from the frequency domain to the time domain, and to write expressions for synthetic seismograms. As the problem is linear, we can use the Fourier transform (see Babich & Pankratova 1973), but the results can also be rewritten in several other useful forms (convolutory form, wave-packet approach, etc.). We shall derive several of these forms, here, starting with the spectral (Fourier transform) method, and discuss them from the seismological point of view. Several forms presented in this section (e.g. the wave packet approach) were shortly discussed even earlier in Červený (1981a, 1983).

For simplicity, we shall use the same symbol U for the wavefield in the time domain which we have used in the frequency domain, but writing $U = U(S, t)$ instead of $U = U(S, \omega)$. The quantity $U(S, t)$ may again be either a scalar or a vector quantity.

We denote the source-time function by $f(t)$ and assume that $f(t)$ is absolutely integrable. We understand that $f(t)$ corresponds to the far-field approximation. We denote the spectrum

of $f(t)$ by $F(\omega)$,

$$f(t) = \frac{1}{\pi} \operatorname{Re} \int_0^\infty F(\omega) \exp(-i\omega t)\, d\omega. \tag{11}$$

We also assume that $f(t)$ is a high-frequency function. This means that the Fourier spectrum $F(\omega)$ of $f(t)$ effectively vanishes for small frequencies,

$$F(\omega) = 0 \qquad \text{for} \qquad 0 \leqslant \omega \leqslant \omega_0, \tag{11'}$$

where ω_0 is high.

4.1 THE SPECTRAL APPROACH

Using the Fourier transform, we obtain

$$U(S, t) = \frac{1}{\pi} \operatorname{Re} \int_0^\infty (-i\omega)^{k/2} F(\omega) \exp(-i\omega t) \int_{\phi_0}^{\phi_N} \int_{\delta_0}^{\delta_M} \Phi(\phi, \delta) \times u(S, \omega, \phi, \delta)\, d\phi d\delta d\omega, \tag{12}$$

from (9). The above expression can be rewritten in the following form (see 1),

$$U(S, t) = \frac{1}{\pi} \operatorname{Re} \int_0^\infty (-i\omega)^{k/2} F(\omega) \int_{\phi_0}^{\phi_N} \int_{\delta_0}^{\delta_N} \Phi(\phi, \delta) A \exp(-\omega G) \times \exp[-i\omega(t-\theta)]\, d\phi d\delta d\omega, \tag{13}$$

where $A = A(s, \phi, \delta)$, $G = G(s, q_1, q_2, \phi, \delta)$, $\theta = \theta(s, q_1, q_2, \phi, \delta)$. Thus, the functions A, G and θ depend on the ray-centred coordinates of point S, corresponding to the selected ray with ray parameters ϕ, δ. In other words, the ray-centred coordinates s, q_1, q_2 depend on ϕ, δ; $s = s(\phi, \delta)$, $q_1 = q_1(\phi, \delta)$, $q_2 = q_2(\phi, \delta)$. The function A depends only on the ray-centred coordinate s, not on q_1 and q_2.

Equation (13) is suitable for computing synthetic seismograms mainly when A also depends on the frequency, e.g. when we consider the frequency-dependent reflection/transmission coefficients from some thin transition layers (see the discussion at the end of Section 2). Equation (13) then gives an approximate high-frequency generalization of the well-known reflectivity method (see Fuchs 1968; Fuchs & Müller 1971) for 2-D and 3-D laterally inhomogeneous layered structures. If A does not depend on the frequency, it will be more effective to use the methods described in Sections 4.2 and 4.3. More details on integral (13) and on its connection with the reflectivity method with some examples of computation will be given elsewhere.

Note that the term $\exp(-\omega G)$ gives some position-dependent windowing of the ray parameters ϕ, δ automatically. Similar windowing of the angle of incidence is also artificially introduced in the reflectivity method.

It should be emphasized that equations (12) and (13) yield the time dependence $f(t)$ in regular ray regions, although the spectrum $F(\omega)$ of $f(t)$ is multiplied by $(-i\omega)^{k/2}$.

4.2 CONVOLUTORY APPROACHES

By changing the order of integrals in (13), we obtain

$$U(S, t) = \operatorname{Re} \int_{\phi_0}^{\phi_N} \int_{\delta_0}^{\delta_M} \Phi(\phi, \delta) A w(S, t, \phi, \delta)\, d\phi d\delta, \tag{14}$$

where

$$w(S, t, \phi, \delta) = \frac{1}{\pi} \int_0^\infty (-i\omega)^{k/2} F(\omega) \exp(-\omega G) \exp[-i\omega(t-\theta)]\, d\omega. \tag{15}$$

To simplify the above expressions, we introduce two new real-valued time functions,

$$x(t) = \frac{1}{\pi} \operatorname{Re} \int_0^\infty (-i\omega)^{k/2} F(\omega) \exp(-i\omega t)\, d\omega,$$

$$h(t) = \frac{1}{\pi} \int_{-\infty}^\infty (\zeta - t)^{-1} x(\zeta)\, d\zeta \tag{16}$$

$$= \frac{1}{\pi} \operatorname{Im} \int_0^\infty (-i\omega)^{k/2} F(\omega) \exp(-i\omega t)\, d\omega.$$

The relation between $x(t)$ and $f(t)$ is controlled by the integer k. For example, for $k = 2$, $x(t)$ is the time derivative of $f(t)$, $x(t) = df(t)/dt$. For $k = 1$, the relation between $x(t)$ and $f(t)$ is as follows:

$$x(t) = \pi^{-1/2} \frac{d}{dt} [H(t)\, t^{-1/2} * f(t)] = \pi^{-1/2} H(t)\, t^{-1/2} * df(t)/dt,$$

where $H(t)$ is the Heaviside function. As we can see from (16), $h(t)$ is the Hilbert transform of $x(t)$. Using this notation, (15) can be rewritten in the two following forms:

$$w(S, t, \phi, \delta) = x(t) * \frac{1}{\pi} \frac{1}{G + i(t-\theta)}, \tag{17}$$

or, alternatively,

$$w(S, t, \phi, \delta) = \hat{x}(t) * \frac{1}{\pi} \operatorname{Im} \frac{1}{t - \theta - iG}, \tag{18}$$

where Im denotes the imaginary part. In (18), $\hat{x}(t)$ is the analytical signal corresponding to the function $x(t)$ (see Bracewell 1965),

$$\hat{x}(t) = x(t) + ih(t). \tag{19}$$

Inserting (17) into (14) yields a useful formula,

$$U(S, t) = x(t) * \frac{1}{\pi} \int_{\phi_0}^{\phi_N} \int_{\delta_0}^{\delta_M} \operatorname{Im} \frac{\Phi A}{t - \theta - iG}\, d\phi d\delta. \tag{20}$$

Similarly, equation (18) with (14) gives

$$U(S, t) = \operatorname{Re} \left\{ \hat{x}(t) * \frac{1}{\pi} \int_{\phi_0}^{\phi_N} \int_{\delta_0}^{\delta_M} \Phi A \operatorname{Im} \frac{1}{t - \theta - iG}\, d\phi\, d\delta \right\}. \tag{21}$$

Alternatively we can write equation (21) in the following form:

$$U(S, t) = x(t) * \frac{1}{\pi} \int_{\phi_0}^{\phi_N} \int_{\delta_0}^{\delta_M} \frac{G \operatorname{Re}(\Phi A)}{(t-\theta)^2 + G^2}\, d\phi d\delta$$

$$- h(t) * \frac{1}{\pi} \int_{\phi_0}^{\phi_N} \int_{\delta_0}^{\delta_M} \frac{G \operatorname{Im}(\Phi A)}{(t-\theta)^2 + G^2}\, d\phi d\delta. \tag{22}$$

As we can see from equations (20)–(22), the oscillatory integrals of the spectral method are replaced by non-oscillatory integrals, which it is simple to compute.

The integrals presented in this section have many properties similar to those of the slowness method discussed in detail by Chapman (1978) and of the disc ray theory (Wiggins 1976). They are, however, applicable to general 2-D and 3-D laterally inhomogeneous structures. They also remain valid in the limiting case of infinitely broad Gaussian beams, $G \to 0$.

The expression $\mathrm{Im}(t-\theta-iG)^{-1} = G[(t-\theta)^2 + G^2]^{-1}$ in the integrands of (21) and (22) approaches for $G \to 0$ the delta function and the integrals lead to simple analytical expressions. For a detailed discussion of similar integrals refer to Chapman (1978) and Chapman & Drummond (1983).

4.3 THE WAVE-PACKET APPROACH

Equation (14) can be rewritten in the following form:

$$U(S, t) = \int_{\phi_0}^{\phi_N} \int_{\delta_0}^{\delta_M} g(S, t, \phi, \delta)\, d\phi d\delta, \tag{23}$$

where

$$g(S, t, \phi, \delta) = \frac{1}{\pi} \mathrm{Re} \left\{ \Phi \int_0^{\infty} (-i\omega)^{k/2} F(\omega) A \exp(-\omega G) \exp[-i\omega(t-\theta)]\, d\omega \right\}. \tag{24}$$

We can call function $g(S, t, \phi, \delta)$ the wave packet. It propagates from the source along the ray specified by ray parameters ϕ, δ and is effectively limited both in space and in time. We remind that $f(t)$ is a high-frequency function. Consequently, $g(S, t, \phi, \delta)$ is a high-frequency packet.

Similar to equation (10), we can again write a discrete form of (23), assuming that the function $g(S, t, \phi, \delta)$ is sufficiently smooth for a given S and t,

$$U(S, t) = \sum_{i=0}^{N} \sum_{j=0}^{M} g(S, t, \phi_i, \delta_j)\, \Delta\phi_i\, \Delta\delta_j, \tag{25}$$

where ϕ_i, δ_j, $\Delta\phi_i$ and $\Delta\delta_j$ have the same meaning as in (10).

The physical explanation of (25) is as follows: The wave packets $g(S, t, \phi_i, \delta_j)$ are emitted from the source into directions ϕ_i, δ_j ($i = 0, 1, \ldots, N$; $j = 0, 1, \ldots, M$). These wave packets propagate along rays specified by parameters ϕ_i, δ_j. They change their properties continuously due to diffusion, spreading, reflections, etc. The resulting synthetic seismogram $U(S, t)$ at any point S of the medium is then obtained as a superposition of the wave packets which 'fly' in the close neighbourhood of the observation point S. It should be emphasized that the wave packets are firmly tied to the rays, even if they correspond to a multiply reflected/refracted (possibly converted) wave.

Equation (24) may be applied even if a frequency-dependent A is considered (see the end of Section 2). If A does not depend on frequency, (24) yields

$$g(S, t, \phi, \delta) = \mathrm{Re}\ \{\Phi A w(S, t, \phi, \delta)\}\ , \tag{26}$$

where $w(S, t, \phi, \delta)$ is given by (15).

If the amplitude spectrum $|F(\omega)|$ is very narrow, highly concentrated close to a prevailing frequency $\omega = \omega^*$, we can use (26) approximately even if A is slightly frequency-dependent. We must then put $A = A(\omega^*)$ in (26). In the following, we shall assume that A does not depend on frequency, and, if so, then A corresponds to $A(\omega^*)$.

Alternative forms of (26) are as follows (see 17 and 18),

$$g(S, t, \phi, \delta) = x(t) * \operatorname{Im} \left\{ \frac{1}{\pi} \frac{\Phi A}{t-\theta-iG} \right\} , \tag{27}$$

or

$$g(S, t, \phi, \delta) = \operatorname{Re} \left\{ \hat{x}(t) * \frac{\Phi A}{\pi} \operatorname{Im} \frac{1}{t-\theta-iG} \right\} . \tag{28}$$

From (27), we obtain another useful equation,

$$g(S, t, \phi, \delta) = x(t) * \frac{1}{\pi} \frac{G \operatorname{Re}(\Phi A) + (t-\theta) \operatorname{Im}(\Phi A)}{G^2 + (t-\theta)^2} \tag{29}$$

Similarly, (28) yields,

$$g(S, t, \phi, \delta) = x(t) * \frac{1}{\pi} \frac{G \operatorname{Re}(\Phi A)}{(t-\theta)^2 + G^2} - h(t) * \frac{1}{\pi} \frac{G \operatorname{Im}(\Phi A)}{(t-\theta)^2 + G^2} . \tag{30}$$

Equations (27)–(30) are surprisingly simple, although they are valid for arbitrary multiply reflected/transmitted (possibly converted) body waves propagating in 2-D or 3-D laterally inhomogeneous layered structures. They are also very efficient from a computational point of view.

In the following, we shall consider special cases of two wave packets, which may be useful in applications. The first will be called the delta packet, and the second the Gaussian packet.

4.3.1 Delta packets

Let us now formally consider that $x(t)$ equals the Dirac impulse function, $x(t) = \delta(t)$. (We hope that the fact that we use the symbol δ both for the Dirac function and for one ray coordinate will not prove confusing.) Note that the Dirac function $\delta(t)$ is not a high-frequency wavelet, but it can be used very effectively as an auxiliary function, assuming that, later on, the results will be convolved with a real high-frequency wavelet. We denote the wave packet corresponding to $x(t) = \delta(t)$ by $g_0(S, t, \phi, \delta)$ and call it the 'delta packet'.

For $g_0(S, t, \phi, \delta)$ (29) immediately yields

$$g_0(S, t, \phi, \delta) = \frac{1}{\pi} \frac{G \operatorname{Re}(\Phi A) + (t-\theta) \operatorname{Im}(\Phi A)}{G^2 + (t-\theta)^2} . \tag{31}$$

As we can see from (31), the evaluation of the delta packet is really very simple, when the parameters of the beam (Φ, A, G, θ) are known.

Let us now denote the wavefield $U(S, t)$ for $x(t) = \delta(t)$ by $U_0(S, t)$. From (20) or from (23), we immediately obtain

$$U_0(S, t) = \int_{\phi_0}^{\phi_N} \int_{\delta_0}^{\delta_M} g_0(S, t, \phi, \delta) \, d\phi d\delta , \tag{32}$$

or, in a discrete form,

$$U_0(S, t) = \sum_{i=0}^{N} \sum_{j=0}^{M} g_0(S, t, \phi_i, \delta_j) \, \Delta\phi_i \, \Delta\delta_j . \tag{33}$$

Equations (32) and (33) are some equivalents of 'impulse seismograms', used broadly in seismic prospecting. For a wavefield generated by a source with the source time function

$f(t)$ we then obtain

$$U(S, t) = x(t) * U_0(S, t). \tag{34}$$

Remember that $x(t)$ is different from the source time function $f(t)$!

An alternative form of (31)–(34) can be also useful. Equation (31) can be divided into two terms. The first term has a delta-like symmetrical form, concentrated close to the time $t = 0$. The second term, however, is antisymmetrical and broader. From a computational point of view, the first term has a more suitable form. It is simple to show that (31) can be rewritten as follows

$$g_0(S, t, \phi, \delta) = g_0^{\mathrm{R}}(S, t, \phi, \delta) + \frac{1}{\pi t} * g_0^{\mathrm{I}}(S, t, \phi, \delta), \tag{35}$$

where

$$g_0^{\mathrm{R}} = \frac{1}{\pi} \frac{G\,\mathrm{Re}(\Phi A)}{G^2 + (t-\theta)^2}, \qquad g_0^{\mathrm{I}} = \frac{1}{\pi} \frac{G\,\mathrm{Im}(\Phi A)}{G^2 + (t-\theta)^2}, \tag{36}$$

Both g_0^{R} and g_0^{I} have now a delta-like form, concentrated close to the time $t = 0$. Equation (32) then yields

$$U_0(S, t) = U_0^{\mathrm{R}}(S, t) + \frac{1}{\pi t} * U_0^{\mathrm{I}}(S, t), \tag{37}$$

where

$$U_0^{\mathrm{R}}(S, t) = \int_{\phi_0}^{\phi_N} \int_{\delta_0}^{\delta_M} g_0^{\mathrm{R}}(S, t, \phi, \delta)\, d\phi d\delta,$$

$$U_0^{\mathrm{I}}(S, t) = \int_{\phi_0}^{\phi_N} \int_{\delta_0}^{\delta_M} g_0^{\mathrm{I}}(S, t, \phi, \delta)\, d\phi d\delta. \tag{38}$$

The discrete form of the above integrals is straightforward. Thus, we can evaluate independently the two time series $U_0^{\mathrm{R}}(S, t)$ and $U_0^{\mathrm{I}}(S, t)$, and then convolve the latter with $1/\pi t$. The final result $U(S, t)$ is again given by (34), which can be also rewritten in the form

$$U(S, t) = x(t) * U_0^{\mathrm{R}}(S, t) - h(t) * U_0^{\mathrm{I}}(S, t). \tag{39}$$

4.3.2 Gaussian packets

As was shown above, the wave packets can be computed either by Fourier transform (see 24), or by convolution (see 27–30). Both the procedures are simple and straightforward, especially the procedure based on convolution. It would, however, be useful also to seek some realistic source-time function for which the expressions for the wave packets can be written in an analytical form, even if approximately.

Here we shall describe one such signal for which we can write approximate expressions for the wave packets. Let us consider the wavelet $f(t)$ given by the formula

$$f(t) = \exp\left[-(2\pi f_{\mathrm{M}} t/\gamma)^2\right] \cos(2\pi f_{\mathrm{M}} t + \nu), \tag{40}$$

with three free parameters, f_{M}, γ, ν. Wavelet (40) corresponds to a harmonic carrier with a Gaussian (bell-shaped) envelope. The quantity γ controls the width of the Gaussian envelope, with respect to the prevailing frequency f_{M}. We assume that the prevailing frequency f_{M} is high. The envelope is narrow for small γ and broad for large γ. Wavelet (40) has been

broadly used in ray methods and in computing ray synthetic seismograms. A detailed discussion of the wavelet $f(t)$ can be found, e.g. in Červený *et al.* (1977). Wavelet (40) has also been used in other branches of science, not only in wave propagation problems. Let us mention, e.g. time series processing, holography, etc. It has been known under different names. Examples are the Puzyrev's wavelet, Gabor's wavelet, Gaussian envelope wavelet, etc. It has very interesting properties. For example, it can be differentiated an infinite number of times. It has a smooth, non-oscillating amplitude spectrum highly concentrated close to the prevailing frequency $f = f_M$, especially when γ is high (say, $\gamma > 3$). Similarly as general time records can be decomposed into harmonic components using the Fourier transform, they can also be decomposed into Gabor's wavelets $f(t)$ using so-called Gabor's transformation. For details see Gabor (1946), Bastiaans (1980), Morlet (1981) and Morlet *et al.* (1982). A detailed discussion of Gabor's transformation from the point of view of applications in the processing of seismic data can be found in Morlet *et al.* (1982).

Let us note that the function $f(t)$ given by (40) is not strictly a high-frequency signal, as it does not satisfy (11′). For large γ, however, its spectrum is concentrated close to the high prevailing frequency f_M and its low-frequency components effectively vanish.

Let us now write the expressions for the analytical signal $\hat{f}(t)$ corresponding to $f(t)$. It is given by the expression (see Bracewell 1965),

$$\hat{f}(t) = \frac{1}{\pi} \int_0^\infty F(\omega) \exp(-i\omega t)\, d\omega, \tag{41}$$

where $F(\omega)$ is the Fourier spectrum of $f(t)$. It is easy to see that for large γ we can write approximately

$$\hat{f}(t) \sim \exp[-(2\pi f_M t/\gamma)^2 - i2\pi f_M t - i\nu] \tag{42}$$

(for details see Červený 1976). Equation (42) can be analytically continued even to complex-valued t to yield

$$\hat{f}(t-\theta-iG) \sim \exp[-(2\pi f_M (t-\theta-iG)/\gamma)^2 - i2\pi f_M (t-\theta-iG) - i\nu].$$

This simply leads to the final equation

$$\hat{f}(t-\theta-iG) \sim \exp[-(2\pi f_M (t-\theta)/\gamma)^2 - 4\pi^2 f_M^2 G^2/\gamma^2 - 2\pi f^* G] \times \exp\{-i[2\pi f^*(t-\theta)+\nu]\}, \tag{43}$$

where

$$f^* = f_M \left(1 - \frac{4\pi f_M G}{\gamma^2}\right). \tag{44}$$

Note that (43) is a special case of a more general equation derived by Červený & Frangié (1980) in the connection with the propagation of seismic wavelets in media with a causal absorption.

Let us now write similar expressions for the analytical signal $\hat{x}(t)$ corresponding to $x(t)$ (see 19 and 16), where $F(\omega)$ is the Fourier spectrum of the wavelet (40). If $k = 2$, $\hat{x} = d\hat{f}/dt$ and (43) immediately yields

$$\hat{x}(t-\theta-iG) = -i2\pi f_M [1 + i2\pi f_M (t-\theta-iG)/\gamma^2]\, \hat{f}(t-\theta-iG), \tag{45}$$

where $\hat{f}(t-\theta-iG)$ is given by (43). For $k = 1$, the resulting equation is more complicated. As $\hat{x} = \pi^{-1/2} H(t)\, t^{-1/2} * d\hat{f}(t)/dt$, we obtain

$$\hat{x}(t-\theta-iG) = \pi^{-1/2} H(t) t^{-1/2} * \{-i2\pi f_M [1 + i2\pi f_M (t-\theta-iG)/\gamma^2]\, \hat{f}(t-\theta-iG)\}, \tag{46}$$

where $f(t-\theta-iG)$ is again given by (43). Both formulae can be simplified for larger γ, when we take into account that the amplitude spectrum is strongly concentrated close to the prevaling frequency f_M. Equations (45) and (46), or alternatively (15), then yield

$$\hat{x}(t-\theta-iG) \sim (-i2\pi f_M)^{k/2} f(t-\theta-iG). \tag{47}$$

Using the simple equation (47), the final formula for the Gaussian wave packet $g(S, t, \phi, \delta)$ is as follows,

$$g(S, t, \phi, \delta) = (2\pi f_M)^{k/2} |\Phi A| \exp\{-[2\pi f_M(t-\theta)/\gamma]^2 + 4\pi^2 f_M^2 G^2/\gamma^2 - 2\pi f_M G\}$$

$$\times \cos\{2\pi f^*(t-\theta) + \nu - \arg(\Phi A) + k\pi/4\}. \tag{48}$$

Equation (48) clearly shows that the prevailing frequency of the Gaussian packet is f^* and (44) describes quantitatively the decrease of the prevailing frequency f^* with increasing distance from the central ray. From (44) and (48) immediately follows the decrease of the prevailing frequency of the wavefield for waves penetrating into shadow zones. It should be noted that the approximate equation (48) for the Gaussian packet is valid only in some neighbourhood of the central ray, for which the correction $4\pi^2 f_M^2 G^2/\gamma^2$ in (48) is small with respect to $2\pi f_M G$, i.e. for which $2\pi f_M G/\gamma^2$ is small with respect to unity. A modification of (48) for larger $4\pi^2 f_M^2 G^2/\gamma^2$ was suggested by Klimeš (1982b).

As we can see from (48), the Gaussian packets have an approximately Gaussian envelope both in space and time. The envelope is strictly Gaussian in the time domain and does not change as the wave progresses; see the exponential term $\exp[-(2\pi f_M(t-\theta)/\gamma)^2]$ in (48). In the direction perpendicular to the ray, the envelope is not strictly Gaussian; we have obtained two terms depending on G and G^2 in the expression for the envelope. The term depending on G^2, however, has only the character of a correction, and (48) can only be used from the network of velocity points.

5 Synthetic seismograms by the Gaussian packet approach. Numerical examples

To write programs for the evaluation of synthetic body wave seismograms based on the Gaussian packet approach is even simpler than to write the program for the ray synthetic seismograms. There are two reasons for this: (1) The Gaussian packet approach does not require two-point ray tracing; it is sufficient to compute the rays as an initial-value problem and cover the region where the receivers are situated by these rays. (2) The Gaussian packet approach is not so sensitive to details of the velocity distribution in the model as the ray method, so that simpler approximations can be used to determine the velocity distribution from the network of velocity points.

5.1 A SHORT DESCRIPTION OF THE PROGRAM PACKAGE BEAM 81

A program package, BEAM 81, for evaluating body-wave seismograms by the Gaussian packet approach in a general 2-D laterally inhomogeneous layered structure has been written. A line source of elastic waves perpendicular to the plane of the model is considered. Optionally, a multiplicative amplitude factor is used which converts the source into a point source (see Červený & Pšenčík 1979; Červený 1981c). The source may be situated at any point of the medium. The 2-D radiation pattern of the source may be specified independently for *P*- and *S*-waves. Both vertical and horizontal components (or one of them) can be evaluated.

Interfaces are specified by irregularly distributed grid points. They are approximated by a cubic spline interpolation. The interfaces may optionally have corner points and may be fictititous in certain parts. Various interfaces may also partially coincide. In this way, the models with vanishing layers, block structures, fractures, isolated bodies. etc., can be handled by the program. The surface of the model may also be curved.

The velocity distribution in the individual layers is specified by a 2-D rectangular network covering the whole layer, independently for each layer. The velocity distribution is then determined by a suitable approximation, e.g. by a bicubic spline approximation.

The program package consists of five programs. The first program of the package, also called BEAM 81, is the most extensive. In the program, the numerical codes of elementary waves are successively generated. The generation is semi-automatic, automatically giving all primary reflected waves (including *PS*- and *SP*-waves converted at the reflection point) and refracted waves. Any type of other multiply reflected/refracted wave (which may also be converted) can be generated manually, by the input data.

For each wave, a system of rays with ray parameters ϕ_i, $i = 0, 1, 2, \ldots, N$, is computed by Runge-Kutta's method. The ray parameters can be chosen irregularly to get a more uniform distribution of rays in the investigated region. For all rays with termination points within a specified region of the surface of the Earth, dynamic ray tracing is performed (twice) and all the quantities necessary for evaluating Gaussian beams are stored for all the termination points of the rays. These stored data can be used to compute the synthetic seismograms in any system of receivers distributed regularly or irregularly at the surface within the region under consideration.

The data concerning ray diagrams of individual waves, corresponding travel times and amplitudes can also be optionally stored during the computations for plotting purposes. These plottings can be performed by the program RAYPLOT, another program of the package.

In the program GBDIF, which processes data generated by the program BEAM 81, the system of receivers is specified. The receivers are distributed regularly or irregularly along the Earth's surface. The program determines the contributions of individual Gaussian packets at the receiver points. A simplified approach based on the paraxial ray approximation described in Section 3 is used which determines the Gaussian packets from the quantities stored at the termination points of individual rays along the Earth's surface.

Other input data of the program GBDIF control the initial parameters of Gaussian beams (initial half-width and the initial curvature of the phase front of the beam), the selection of rays from those evaluated in the program BEAM 81 and stored in the computer which are used in the discrete expansion formulae, the windowing function which truncates the theoretically infinite width of Gaussian beams, etc. The windowing is controlled by a parameter a which has the following meaning: only those Gaussian beams are considered at the receiver point, the amplitude of which at the receiver point is larger than a per cent of the amplitude at the corresponding central ray.

Thus, when the file generated in the program BEAM 81 is available, the program GBDIF (with the program BEAMPL described below) allows fast and effective evaluation of synthetic seismograms for different systems of receivers, with different initial parameters of Gaussian beams, with different selection of rays and different windowing of Gaussian beams.

It should be noted that the initial parameter corresponding to the half-width of the Gaussian beam at the source was used in GBDIF in the form suggested by Červený & Pšenčík (1983), i.e. frequency-independent. It corresponds to the same parameter given in Červený *et al.* (1982a) when we put $\omega = 2\pi$.

The file generated in GBDIF can be used to evaluate the Gaussian packet synthetic body-

wave seismograms for various parameters of the source-time function (40) f_M, γ and ν, for a vertical and/or horizontal component, for a specified time interval and a reduction velocity. This can be done in the BEAMPL program. The approximate equation (48) is used for this purpose. The resulting synthetic seismograms are stored in a file, which is used in the SEISPLOT program to plot results (with optical amplitude-distance scaling).

The program package was written and all the computations presented in the following were performed with the VAX11 computer at the Department of Geophysics, Stanford University. The program uses extensively parts of the RAY 81 program for initial-value ray tracing and ray amplitude computation in 2-D media, written by I. Pšenčík (see Pšenčík 1983). Some routines from the SEIS 81 program for evaluating ray synthetic seismograms are also used in the package. Both the RAY 81 and SEIS 81 programs are described by Červený & Pšenčík (1981). Certain results of computations performed by the program package BEAM 81 were presented earlier (see Červený 1981b).

5.2 NUMERICAL EXAMPLES

It would be possible to use the BEAM 81 program package for computing synthetic body-wave seismograms in general 2-D laterally inhomogeneous structures. It is, however, useful to start with investigating simpler situations to see the behaviour of Gaussian packet synthetic seismograms in a more lucid form.

The accuracy of the Gaussian packet approach and its possible dependence on the initial parameters of Gaussian beams (initial half-width and the initial curvature of the phase front of the Gaussian beams at the source) will be investigated in detail elsewhere. Comparisons with more accurate methods (e.g. with the reflectivity method) in types of media, to which these methods can be applied, will be used for this purpose. Here we shall present only a few examples which may give us a better insight into the whole procedure. In all the examples presented here, the initial half-width of the Gaussian beams at the source was chosen close to the optimum value suggested in Červený *et al.* (1982a). Similarly, the initial curvature of the phase front of the beam at the source was chosen equal to 0. As the applications of the Gaussian beam approach in a smooth medium (including the caustic region) was investigated by Červený *et al.* (1982a), our attention will be concentrated on models with interfaces. The simplest possible case is a plane interface between two homogeneous media. Attention will be devoted both to the regions in which the ray field behaves regularly and to singular regions (critical region, etc.). In all the presented examples, we shall consider idealized simplified models of the Earth's crust. The models are 600 km long and 50 km deep. (Only 400 km of the models will be shown in the following pictures, but the region covered by the rays in computations was 600 km long.) A line source of the explosive type with a circular radiation pattern is situated close to the Earth's surface at the horizontal coordinate $x = 200$ km. The source radiates only *P*-waves. A multiplicative amplitude factor is used to convert the line source into a point source. The source-time function is given by (40), with $\gamma = 4$ and $\nu = 0$. (This value of γ is sufficiently high to apply the approximate expression 48.) The prevailing frequency f_M is different in the individual pictures, varying from $f_M = 3$ to 16 Hz.

Only one inner interface is considered in the model. It is situated at a depth of 30 km below the source. In the first example, the interface is a horizontal plane, in the next two examples, a step or a corner point in the interface occurs at $x = 250$ km (i.e. at an epicentral distance of 50 km).

The *P* velocity in the overburden is 6.4 km s^{-1}, in the substratum 8 km s^{-1}. The ratio of compressional-to-shear velocity equals $\sqrt{3}$ in the whole model, and the density ρ is determined from the *P* velocity α by the relation $\rho = 1.7 + 0.2\alpha$.

Only *PP* reflected waves are considered, converted waves are not taken into account.

As mentioned above, the initial half-width L_0 of the Gaussian beams at the source was chosen close to the optimum value in all the examples. The calculated synthetic seismograms depend generally only slightly on the choice of L_0. In regions, in which the ray field behaves regularly, the wavefield is practically independent on L_0. Some slight dependence was obtained in singular regions. Generally, the most accurate results are obtained for larger L_0; the decrease of L_0 causes some smoothing of spatial distribution of amplitudes.

Let us add one remark regarding the head waves. In the ray method, the head waves are not automatically included in the reflected wavefield, they must be evaluated independently. In the Gaussian beam approach, however, the reflected wavefield includes automatically the head waves due to the singularity of the reflection coefficient in the integrand of the expansion integrals discussed above. Special computations (not presented here) with a denser system of rays close to the critical point and with higher values of L_0 gave really even the head waves. No special care was devoted to this problem in the computations presented here, only a regular step in the ray parameter was used outside and inside the critical region. With this regular step, and with the standard value of L_0, the head waves were not obtained. Due to these facts, the results presented here give some slightly smoothed results. The detailed discussions of these problems will be published elsewhere.

First example. Plane interface

In this example, we consider a plane interface and investigate the *PP* reflected wavefield. This is a classical problem of theoretical seismology, broadly discussed in many papers and books. We shall pay attention both to the regular regions and to the singular region (neighbourhood of the critical ray). The ray diagram, the travel-time curve and the ray amplitude–distance curve corresponding to the *PP*-wave are shown in Fig. 1(a, b, c). To make Fig. 1(a–c) more consistent with the synthetic seismograms presented later, the two-point ray

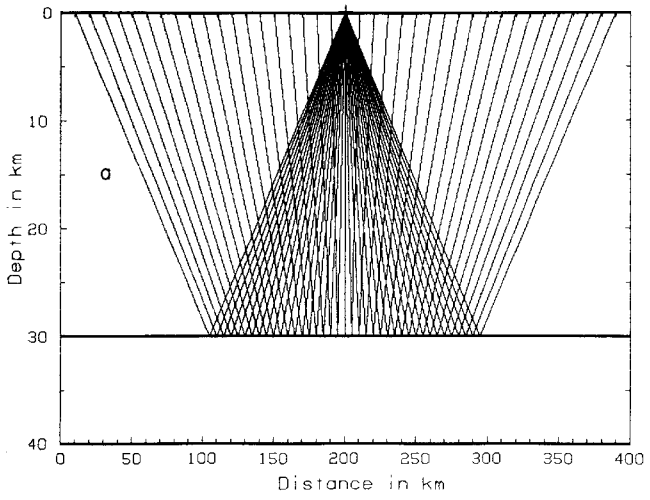

Figure 1. (a) A simple model with a plane interface used for the computation of synthetic seismograms of reflected *PP*-waves in Figs 2–6. The source is situated at the horizontal distance $x = 200$ km. The ray diagram of reflected waves is quite regular. (b) Travel times of reflected *PP*-waves for the model shown in (a). (c) Ray amplitudes of reflected *PP*-waves for the model shown in (a). The increase of amplitudes at epicentral distances of 80 km ($x = 120$ and 280 km) corresponds to critical regions.

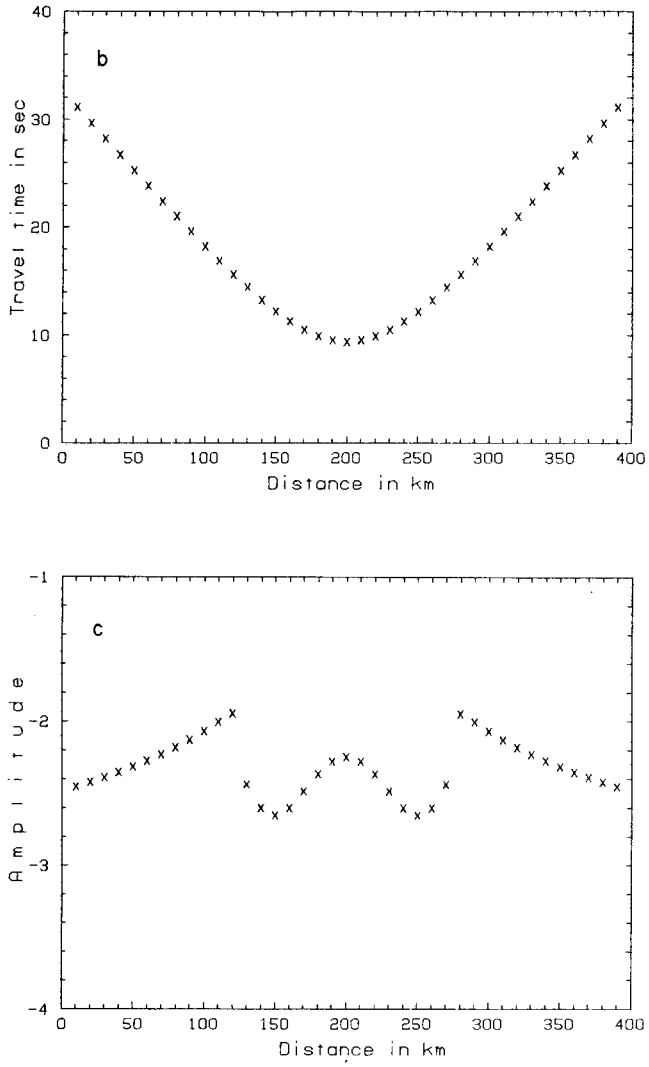

Figure 1 – *continued*

tracing was used to obtain the regular distribution of termination points along the Earth's surface in these pictures. (In actual Gaussian packet synthetic seismogram computations, initial value ray tracing was, of course, used.) The travel-time curve has the well-known hyperbolic form. Similarly, the form of the amplitude–distance curve is also well known. The only, but important singularity in the amplitude–distance curve is connected with the critical region. The critical points in our model are situated symmetrically on either side of the source, at epicentral distances of 80 km, i.e. at $x = 120$ and 280 km. With increasing epicentral distance, the ray amplitudes of reflected *PP*-waves slowly and smoothly decrease at small epicentral distances, they then increase abruptly before reaching the critical point and attain a maximum value just at the critical point. After this, they again decrease slowly. It is well known from comparisons with exact computations that the ray method does not give correct results in the critical region. The maximum of the amplitude–distance curve

computed by more accurate method is not situated at the critical point, but is shifted beyond the critical point, the shift being frequency-dependent. The amplitude distance curve is smooth even at the critical point. For details see Červený & Ravindra (1971) and Červený *et al.* (1977).

Fig. 2 shows the formation of the synthetic body-wave seismograms by superposition of Gaussian packets. The prevailing frequency f_M equals 3 Hz. The synthetic seismograms are shown on a reduced time-scale, with the reduction velocity $v_R = 7\,\mathrm{km\,s^{-1}}$. The reduced time-scale transforms the hyperbolic travel-time curves into a symmetrical curve with the maximum at zero epicentral distance. The synthetic seismograms cover both the normal incidence and the critical region.

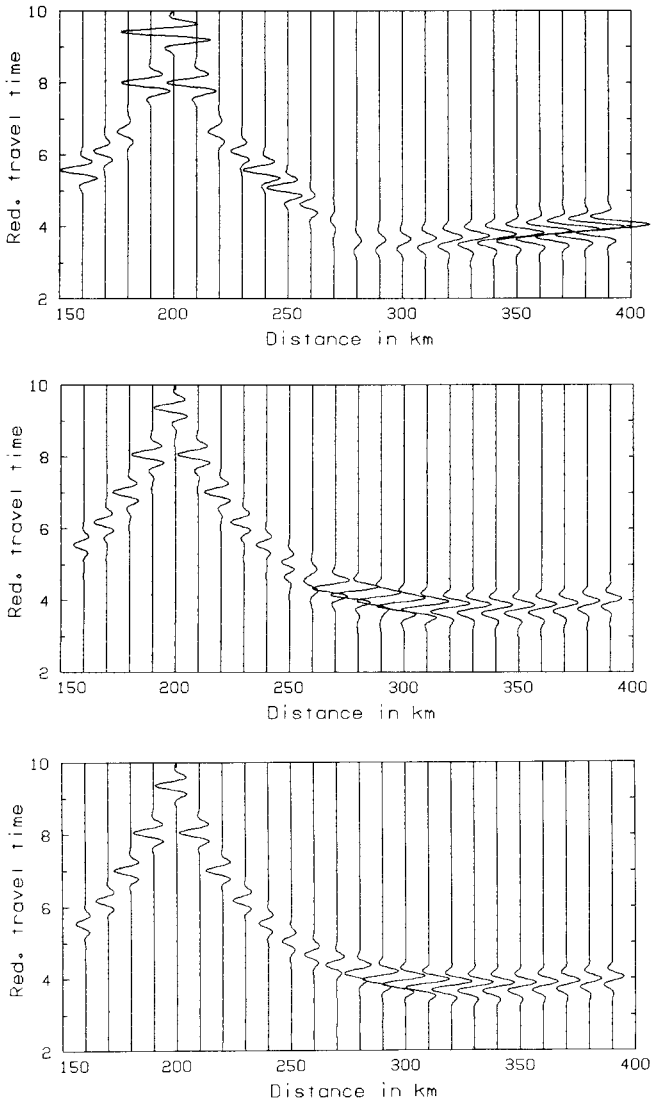

Figure 2. Gaussian packet synthetic seismograms of reflected *PP*-waves for the model shown in Fig. 1(a). The prevailing frequency is $f_M = 3$ Hz, the reduction velocity $v_R = 7\ \mathrm{km\,s^{-1}}$. The number of Gaussian packets covering the whole region is four in the top picture, 16 in the middle picture, and 64 in the bottom picture.

In the top picture, the whole region of interest was covered just by four Gaussian beams. In the picture it is clearly seen that the number of Gaussian packets is not yet sufficient to form the reflected wavefield. In the middle picture, the number of Gaussian packets was increases four times, to 16 packets. The synthetic seismograms look better, the individual Gaussian packets form a continuous wavefield. The number of packets, however, is not yet sufficient. The bottom picture shows the synthetic seismograms constructed from 64 Gaussian packets. They give an excellent numerical agreement to three or four valid digits with the ray synthetic seismograms in regular regions (normal incidence and its vicinity) and a good description of the wavefield in the critical region. The amplitude maximum is shifted from the epicentral distance of 80 km to about 100 km (i.e. $x = 300$ km), which corresponds fully to exact computations. (Note that a picture practically identical to the bottom one was obtained even from 32 packets.)

Thus, we can see that the evaluation of only 30–60 packets was quite satisfactory for the computations of synthetic seismograms in over a 250 km range of epicentral distances (for a prevailing frequency of 3 Hz). To be more precise, several packets were added with the termination points outside the range covered by the receivers.

The following pictures are devoted to a more thorough investigation of the critical region, for epicentral distances ranging from 50 km ($x = 250$ km) to 150 km ($x = 350$ km). The reduction velocity v_R is again $v_R = 7.0\ \mathrm{km\ s^{-1}}$. Fig. 3 shows the comparison of the ray synthetic seismograms (top) with the Gaussian packet seismograms (bottom) for a prevailing

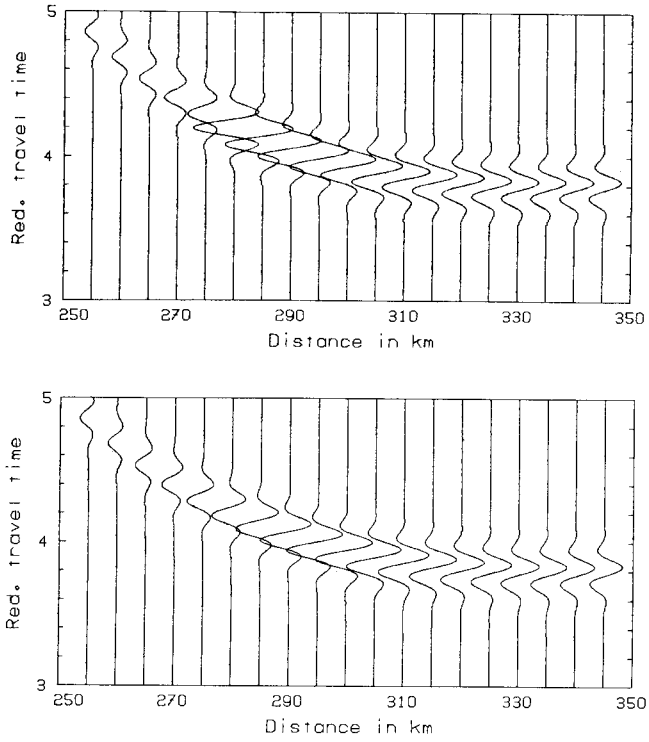

Figure 3. Comparison of ray synthetic seismograms (top picture) and the Gaussian packet synthetic seismograms of reflected *PP*-waves in the critical region for the model shown in Fig. 1(a). The prevailing frequency is $f_M = 4$ Hz, the reduction velocity $v_R = 7\ \mathrm{km\ s^{-1}}$. While the ray synthetic seismograms have a sharp amplitude maximum at the critical distance of 80 km from the source ($x = 280$ km), the maximum amplitudes in the Gaussian packet synthetic seismograms are shifted to distances of ~100 km from the source ($x = 300$ km).

frequency of $f_M = 4$ Hz. All the above discussed pecularities of the wavefield in the critical region are clearly seen in both pictures. While the ray seismogram is anomalous at the critical point ($x = 280$ km), the Gaussian packet seismogram is quite regular at this point and the maximum amplitudes are shifted to a distance of $x = 300$ km, which corresponds to the more accurate computations.

The shift of the maximum of the amplitude–distance curve is frequency-dependent. Fig. 4 shows Gaussian packet synthetic seismograms for various prevailing frequencies, $f_M = 4$, 10 and 16 Hz. As we can see, the shift is the larger, the smaller the frequency.

It is obvious that a larger number of Gaussian packets must be evaluated to obtain

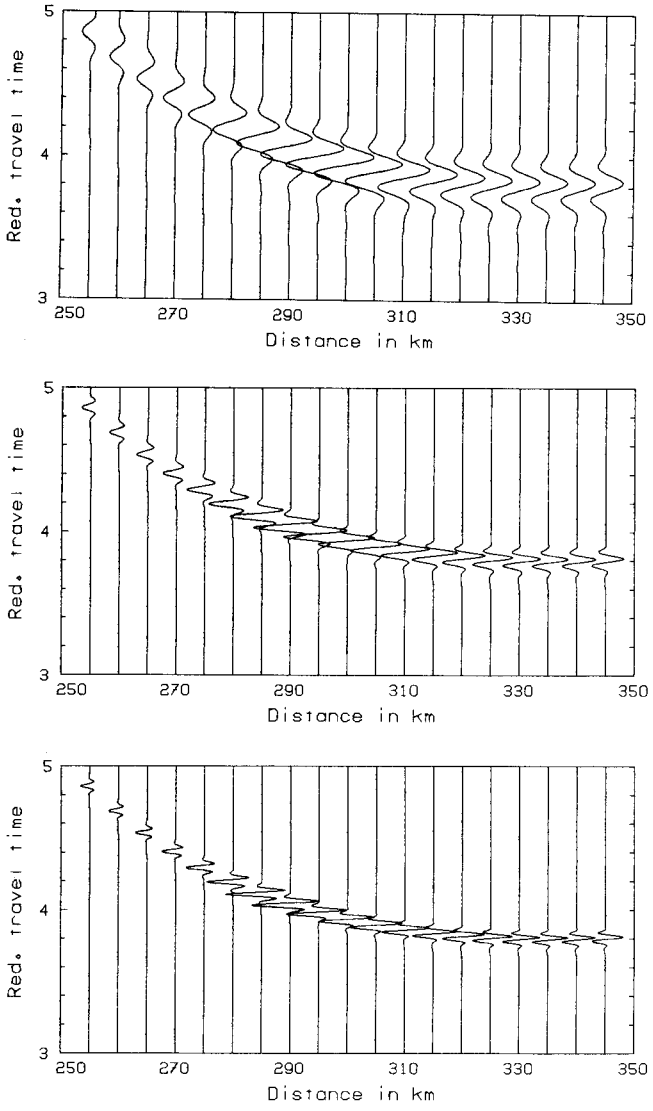

Figure 4. Gaussian packet synthetic seismograms of reflected *PP*-waves in the critical region for the model shown in Fig. 1(a). The reduction velocity is $v_R = 7$ km s^{-1}. The prevailing frequency f_M equals 4 Hz in the top picture, 10 Hz in the middle picture and 16 Hz in the bottom picture. The frequency behaviour of synthetic seismograms in the critical region is clearly seen in the pictures.

smooth synthetic seismograms for higher prevailing frequencies. Fig. 5 shows how the high-frequency body wave synthetic seismograms are formed by the superposition of Gaussian packets, when the frequency is really high (f_M = 16 Hz). In the first picture (Fig. 5a), we can see just one packet and some small parts of two other packets, with the central rays outside the range of interest. The resulting seismogram, of course, does not resemble anything useful and is very far from the exact synthetic seismogram. The number of Gaussian packets was successively doubled from one picture to another. Even in Fig. 5(d), constructed approximately with 24 packets, the number of packets is not sufficient due to the high prevailing

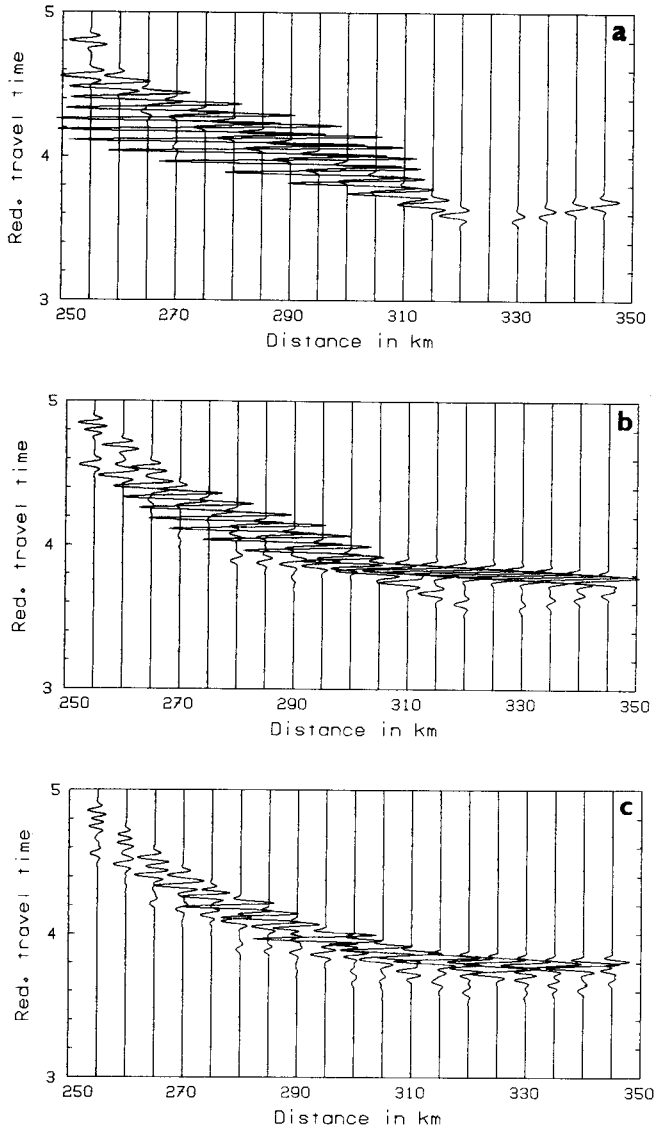

Figure 5. Gaussian packet synthetic seismograms of reflected *PP*-waves in the critical region for the model shown in Fig. 1(a). The reduction velocity v_R = 7 km s^{-1}, the prevailing frequency f_M = 16 Hz. The number of Gaussian packets covering the whole region is successively doubled from one picture to another. It equals 2–3 in 5(a) and close to 50–100 in 5(f).

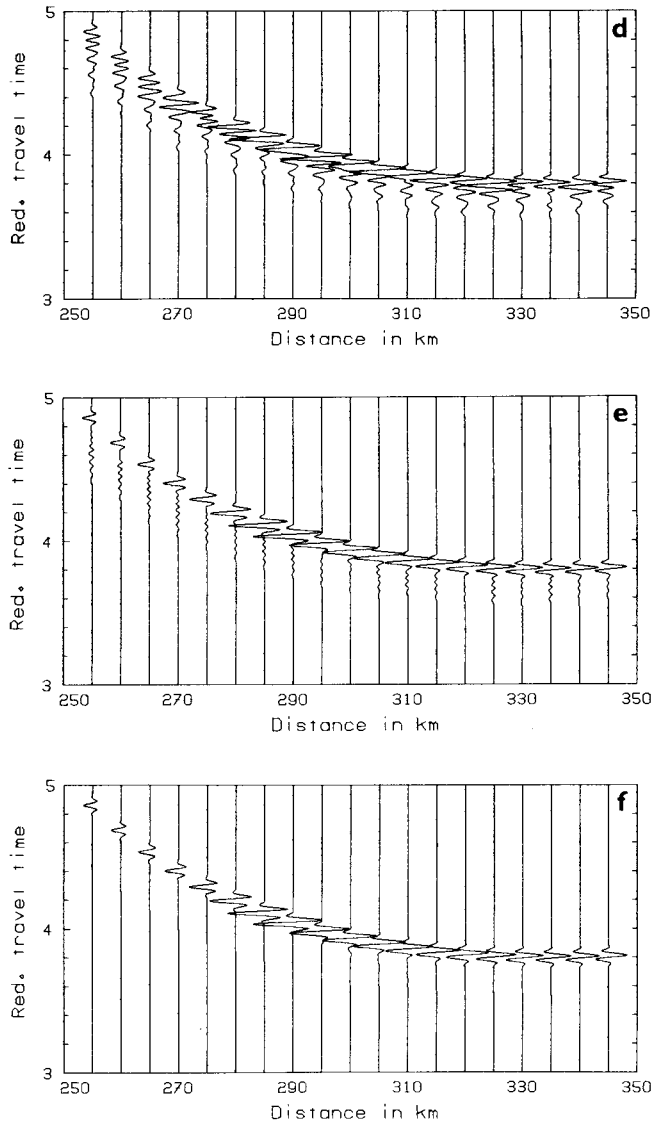

Figure 5 – *continued*

frequency. For 48 packets, the results look well but some small non-causal oscillations still appear in the picture. Finally, in Fig. 5(f), the resulting synthetic seismogram is quite clean.

It is clear that the Gaussian packet may be effectively truncated at some distance from the central ray, where its amplitude is negligibly small in comparison with the amplitude on the central ray. Fig. 6 shows three systems of Gaussian packet seismograms for the prevailing frequency $f_M = 4$ Hz, constructed with different values of a. (The parameter a controls the width of the windowing, see Section 5.1.) In the top picture, $a \sim 13$ per cent, in the middle picture $a \sim 37$ per cent and in the bottom picture, $a \sim 50$ per cent. We can see that all three synthetic seismograms are very similar, at least from an interpretational point of view. This is a very surprising result: only a narrow, central part of the Gaussian packet can be used to obtain satisfactory results. This fact, of course, increases the effectiveness of the method. The

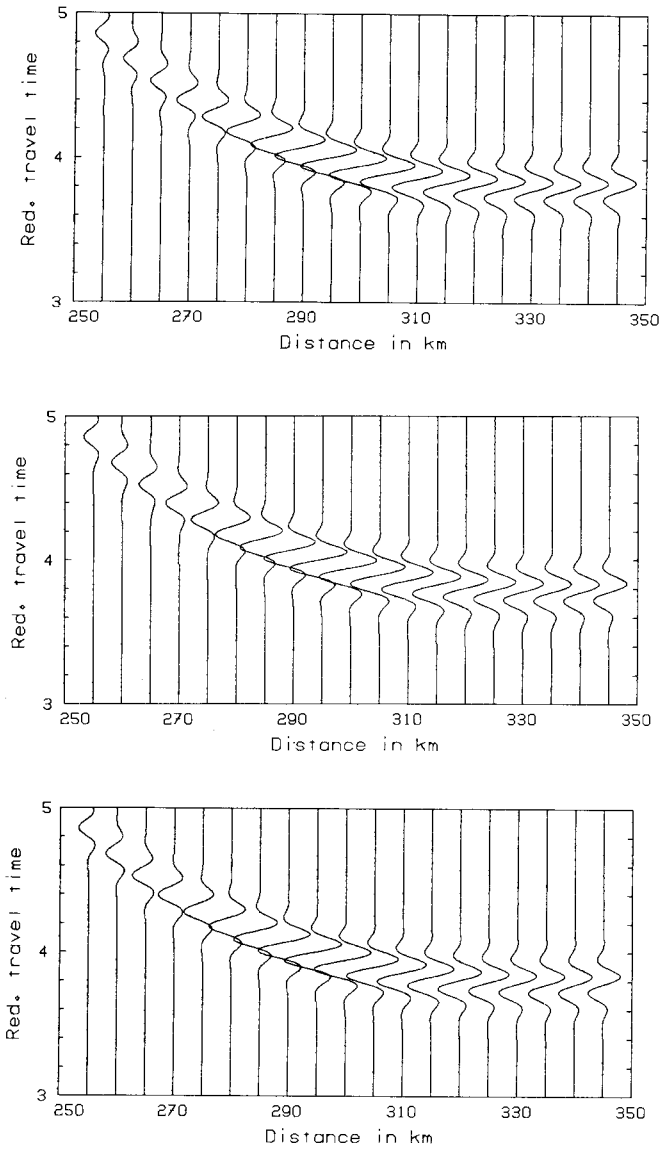

Figure 6. Gaussian packet synthetic seismograms of reflected *PP*-waves in the critical region for the model shown in Fig. 1(a). The reduction velocity v_R = 7 km s^{-1}, the prevailing frequency f_M = 4 Hz. The figure shows a small effect on the synthetic seismogram of windowing of Gaussian packets. In the top picture, only a slight windowing is applied, in the bottom picture the windowing is very strong, only narrow parts of Gaussian packets close to the central rays are used for computation. For details see text.

physical reason for this behaviour consists in the destructive interference of remote Gaussian beams, discussed in Section 3.

There is still a large number of other important questions regarding the sensibility of the Gaussian packet approach to some other quantities (initial half-width of the beam, initial curvature of the phase front of the beam, etc.). More detailed results, both in the time and frequency domain, will be published elsewhere.

Second example. A block structure

A model similar to that in the first example is also considered in this example, only a step in the interface has been introduced at $x = 250$ km. In this way, a simple block structure is formed; the reflections from the continuation of the interface beyond the step are not considered (see the ray diagram in Fig. 7).

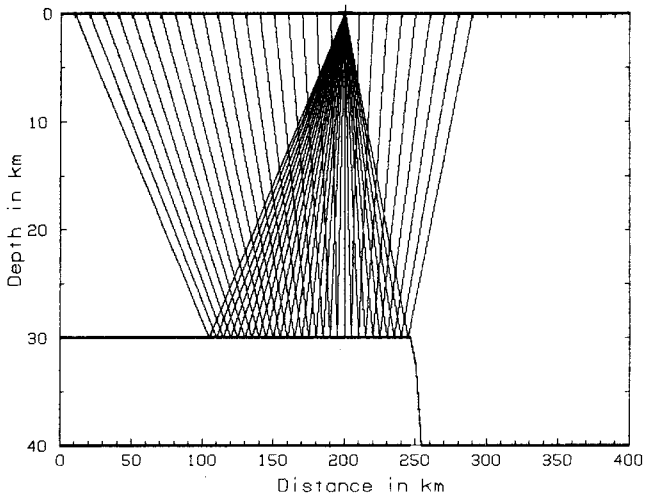

Figure 7. A simple block structure used for computation of synthetic seismograms of reflected *PP*-waves in Figs 8 and 9. As can be seen from the ray diagram, an extensive shadow zone is formed due to the step in the interface.

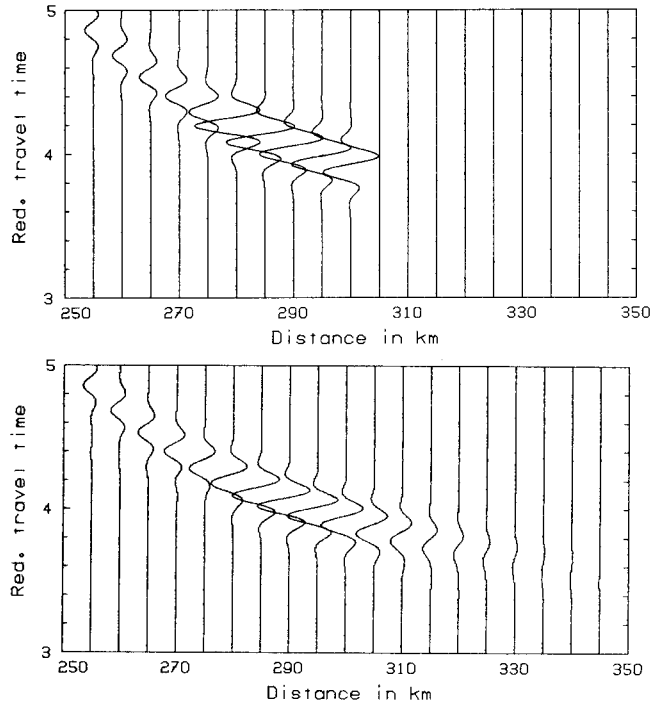

Figure 8. Comparison of ray synthetic seismograms (top picture) and the Gaussian packet synthetic seismograms (bottom picture) of reflected *PP*-waves for the model shown in Fig. 7. The range of distances covers both the critical region ($x \sim 280$ km) and the transition zone between the illuminated region and shadow ($x \sim 300$ km).

The comparison of the ray synthetic seismograms and Gaussian packet seismograms for this model is shown in Fig. 8 for the prevaling frequency $f_M = 4$ Hz. The top picture shows the ray synthetic seismograms, the bottom the Gaussian packet synthetic seismograms. As we can see from Fig. 7, the ray method yields a sharp boundary between the illuminated and shadow zone for the reflected wavefield at distance $x > 300$ km, as no rays exist at $x > 300$ km. The Gaussian packets, however, give a smooth wavefield in this region. Some energy penetrates even into the shadow zone. Of course, the amplitudes decrease rapidly with increasing distance from the boundary to the shadow zone. The decrease of amplitudes is frequency-dependent. Fig. 9 shows synthetic seismograms evaluated for the same model as

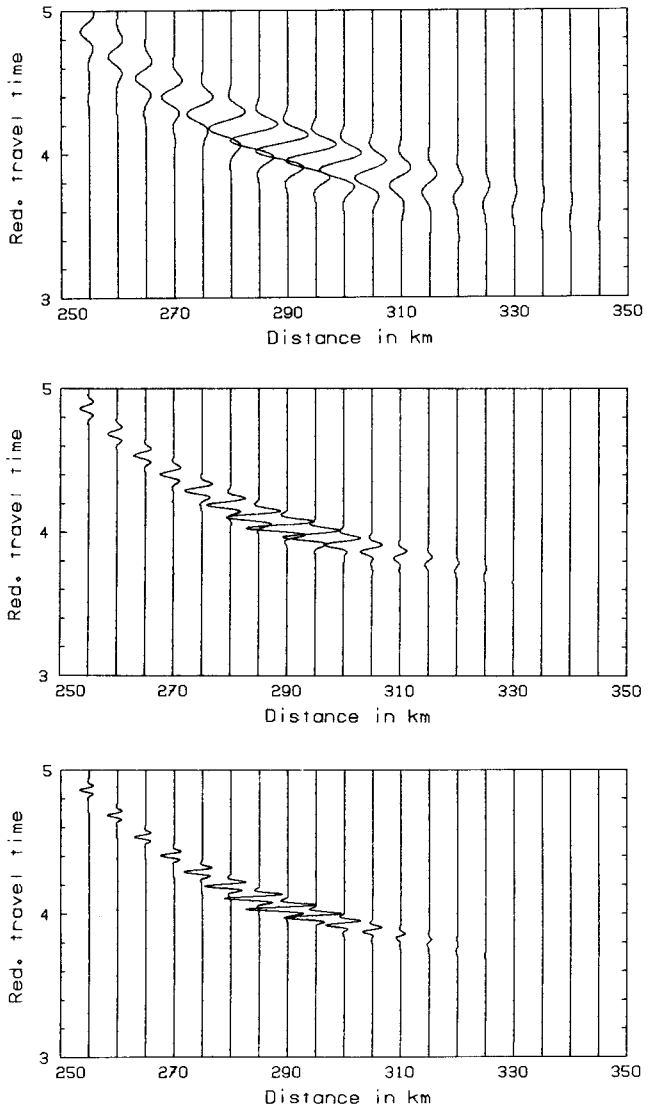

Figure 9. Gaussian packet synthetic seismograms of reflected *PP*-waves for the model of a simple block structure shown in Fig. 7. The reduction velocity $v_R = 7$ km s^{-1}. The prevailing frequency f_M equals 4 Hz in the top picture, 10 Hz in the middle picture and 16 Hz in the bottom picture. The frequency-dependent behaviour of the synthetic seismograms both in the critical region and in the transition zone between the illuminated region and the shadow is clearly seen in the figure.

above, for three prevailing frequencies, $f_M = 4$, 10 and 16 Hz. It can be clearly seen that the decrease of amplitudes into the shadow zone is faster for higher frequencies.

No attempt has been made to compare our results with exact computations. In any case, it can be concluded from the presented pictures that the Gaussian packet approach gives more satisfactory results than the standard ray theory.

It should be noted that the model of the block structure presented here cannot be, strictly speaking, constructed as a superposition of simple Gaussian packets described above. It would be necessary to consider the diffraction of Gaussian packets whose central rays are close to the diffraction (edge) point. The presented results, however, show that even without considering the diffraction of Gaussian packets the method yields promising results.

Third example. Corner at the interface

The object of this example is to show that the Gaussian packet approach is not as sensitive to the approximation of the medium as the ray method. We shall present the results of just two simple computations for the corner at the interface. The corner is situated at an epicentral distance of 50 km ($x = 250$ km).

In Fig. 10, the model and ray diagram are shown. The interface beyond the corner is dipping. Due to the corner, a small shadow zone is formed close to epicentral distances of 105–110 km ($x = 305$–310 km). The ray synthetic seismogram (top) and Gaussian packet seismograms (bottom) for this model are shown in Fig. 11. The shadow zone is clearly seen in the ray synthetic seismograms. The Gaussian packets, however, give more realistic pictures. The amplitudes in this artificial shadow zone, of course, decrease, but the wavefield is smooth.

Fig. 12 shows another model with the corner point at the interface. The interface behind the corner point is rising. The ray diagram shows two branches of rays with a short overlapping region close to the epicentral distance of 95 km ($x = 295$ km). Fig. 13 again shows the ray synthetic seismograms (top) and the corresponding Gaussian packet seismograms

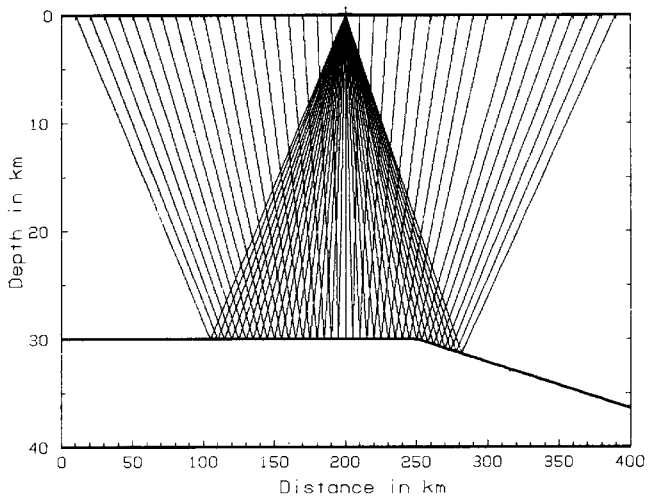

Figure 10. A simple model with a corner in a plane interface used for computing synthetic seismograms of reflected *PP*-waves in Fig. 11. The source is situated at $x = 200$ km. As can be seen in the ray diagram, a small shadow zone due to the corner point is formed at $x \sim 300$ km.

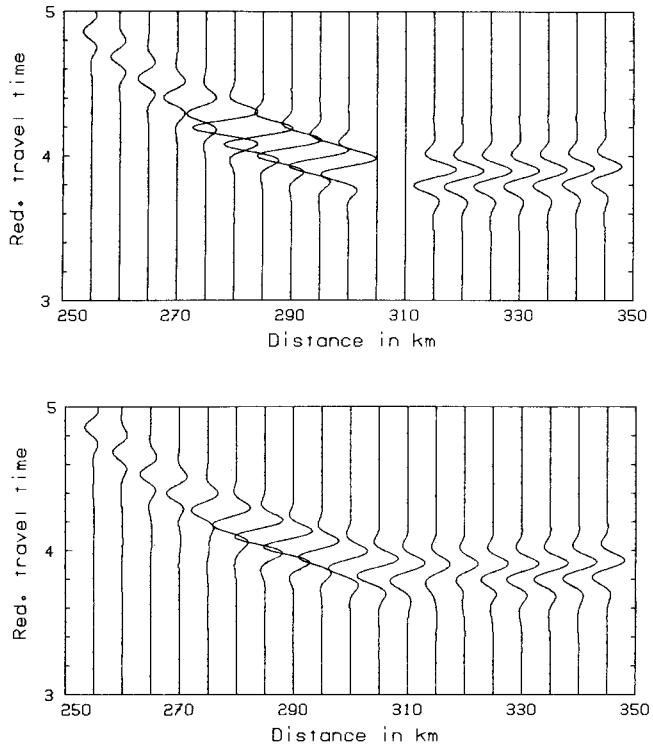

Figure 11. Comparison of ray synthetic seismograms (top picture) and Gaussian packet synthetic (seismograms (bottom picture) of reflected *PP*-waves for the model shown in Fig. 10. The Gaussian packet approach yields a smooth wavefield even in the shadow region cause by the corner point in the interface.

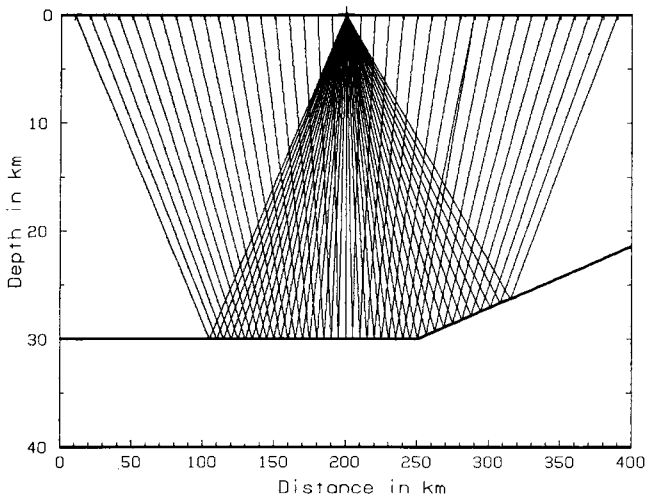

Figure 12. A simple model with a corner point in a plane interface used for the computation of synthetic seismograms of reflected *PP*-waves in Fig. 13. The source is situated at $x = 200$ km. Two branches of the reflected wave overlap in an inextensive zone close to $x \sim 295$ km.

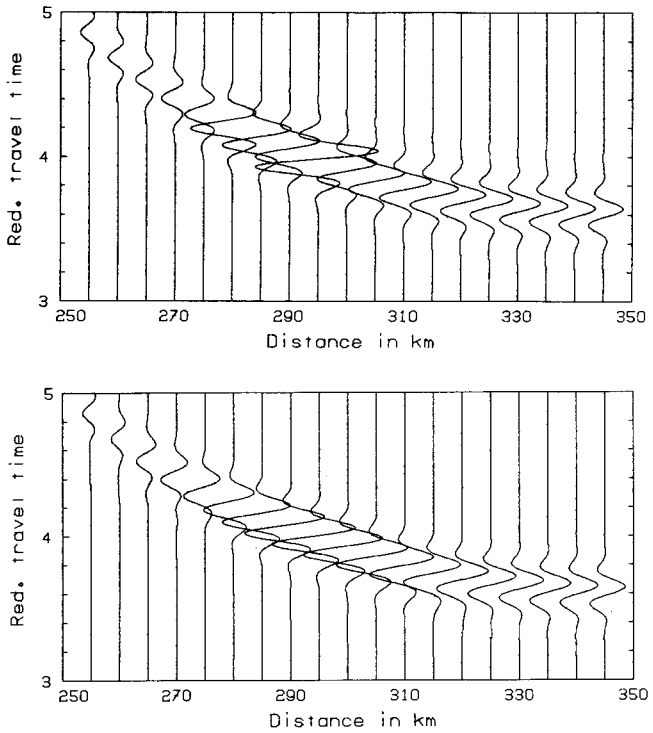

Figure 13. Comparison of ray synthetic seismograms (top picture) and the Gaussian packet synthetic seismograms (bottom picture) of reflected *PP*-waves in the model shown in Fig. 12. The amplitude of the ray synthetic seismogram at $x \sim 295$ km is doubled due to the overlapping of two branches of reflected waves. The Gaussian packet approach smooths this increase caused by the corner point in the interface.

(bottom). Due to the overlapping, the ray amplitudes are approximately doubled at $x = 295$ km in the ray synthetic seismograms. The Gaussian packets give smooth synthetic seismograms, without any substantial increase of amplitudes close to $x = 295$ km. The amplitudes as a whole, of course, increase as the interface beyond the corner point rises.

These two last models show that the approximation of the medium does not play such an important role in the evaluation of Gaussian packet seismograms as it plays in the case of ray synthetic seismograms.

Acknowledgments

The author is greatly indebted to the Stanford Exploration Project and personally to its Director, Professor Jon F. Claerbout, for his invitation to work for 3 months in 1981 at the Department of Geophysics of Stanford University and for valuable and very useful discussions on the subject of Gaussian beams. During this stay, the program package BEAM 81 was written and all the computations presented in this paper were performed. He is also very grateful to many colleagues from various universities and institutions, mainly to Professors K. Aki, L. B. Felsen, J. B. Keller and F. Muir, Drs P. Hubral, M. M. Popov, K. D. Klem-Musatov and G. Nolet for very useful discussions and comments on the problem of Gaussian beams and Gaussian packets. Special thanks are due to Dr I. Pšenčík, for every-day discussions of the Gaussian beam approach and valuable comments concerning the manuscript.

References

Aki, K. & Richards, P., 1980. *Quantitative Seismology*, W. H. Freeman, San Francisco.

Azbel, I. Y., Dmitrieva, L. A. & Yanovskaya, T. B., 1980. The technique for calculation of geometrical spreading in three-dimensional media, in *Computational Seismology, Vol. 13*, pp. 113–127, Nauka, Moscow (in Russian).

Babich, V. M., 1968. Eigenfunctions, concentrated in the vicinity of closed geodesics, in *Mathematical Problems of Theory of Propagation of Waves, Vol. 9*, pp. 15–63, Nauka, Leningrad (in Russian).

Babich, V. M. & Buldyrev, N. J., 1972. *Asymptotic Methods in Problems of Diffraction of Short Waves*, Nauka, Moscow (in Russian).

Babich, V. M. & Kirpichnikova, N. J., 1974. *The Boundary Layer Method in Diffraction Problems*, Leningrad University Press (in Russian, English translation by Springer-Verlag, 1980).

Babich, V. M. & Pankratova, T. F., 1973. On discontinuities of the Green function of mixed problems for wave equation with variable coefficients, in *Problems of Mathematical Physics, Vol. 6*, pp. 9–27, Leningrad University Press (in Russian).

Babich, V. M. & Popov, M. M., 1981. Propagation of concentrated acoustical beams in a three-dimensional inhomogeneous medium, *Akust. Zh.*, **27**, 823–835 (in Russian).

Bastiaans, M. J., 1980. Gabor's expansion of a signal into Gaussian elementary signals, *Proc. I.E.E.E.*, **68**, 538–539.

Born, M. & Wolf, E., 1968. *Principles of Optics*, Pergamon Press, Oxford.

Bracewell, R., 1965. *The Fourier Transform and its Applications*, McGraw-Hill, New York.

Buchen, P. W. & Haddon, R. A. W., 1981. Isochronal formulation of seismic diffraction, in *Identification of Seismic Sources – Earthquake or Underground Explosion*, pp. 373–381, Reidel, Dordrecht.

Cassell, B. R., 1982. A method for calculating synthetic seismograms in laterally varying media, *Geophys. J. R. astr. Soc.*, **69**, 339–354.

Červený, V., 1976. Approximate expressions for the Hilbert transform of a certain class of functions and and their applications in the ray theory of seismic waves, *Studia geophys. geod.*, **20**, 125–132.

Červený, V., 1979. Ray theoretical seismograms for laterally varying structures, *J. Geophys.*, **46**, 335–342.

Červený, V., 1981a. *Seismic Wave Fields in Structurally Complicated Media (Ray and Gaussian Beam Approaches)*, Lecture Notes, Rijksuniversiteit Utrecht, Vening-Meinesz Laboratory, Utrecht.

Červený, V., 1981b. Ray tracing by Gaussian beams, presented at *51st ann. meet. SEG, October 11–15, 1981*, Los Angeles.

Červený, V., 1981c. Dynamic ray tracing in 2-D media (pp. 21–30). Determination of second derivatives of travel-time fields by dynamic ray tracing (pp. 31–38). Ray tracing in a vicinity of a central ray (pp. 39–48). Computation of geometrical spreading by dynamic ray tracing (pp. 49–60). Dynamic ray tracing across curved interfaces (pp. 61–73), in *Stanford Exploration Project, Rep. No. 28*, Department of Geophysics, Stanford University.

Červený, V., 1982. Expansion of a plane wave into Gaussian beams, *Studia geophys. geod.*, **26**, 120–131.

Červený, V., 1983. Computation of synthetic seismograms for 1-D and 2-D inhomogeneous media, in *Numerical Methods in the Interpretation of Seismic Data, Suzdal 1980*, Nauka, Novosibirsk, in press (in Russian).

Červený, V., Popov, M. M. & Pšenčík, I., 1982a. Computation of wavefields in inhomogeneous media – *Studia geophys. geod.*, **24**, 365–372.

Červený, V., Fuchs, K., Müller, G. & Zahradník, J., 1981. Theoretical seismograms for inhomogeneous media, in *Problems of the Dynamic Theory of Propagation of Seismic Waves, Vol. 20*, pp. 84–109, Nauka, Leningrad (in Russian).

Červený, V. & Hron, F., 1980. The ray series method and dynamic ray tracing systems for 3-D inhomogeneous media, *Bull. seism. Soc. Am.*, **70**, 47–77.

Červený, V., Klimeš, L. & Pšenčík, I., 1982. Synthetic seismic wave fields for 2-D and 3-D inhomogeneous structures, in *Proc. 27th int. Geophys. Symp. A(I), Bratislava 1982*, pp. 17–28, Geofyzika n.p., Brno.

Červený, V., Molotkov, I. A. & Pšenčík, I., 1977. *Ray Method in Seismology*, Karlova Universita, Praha.

Červený, V., Popov, M. M. & Pšenčík, I., 1982a. Computation of wave fields in inhomogeneous media – Gaussian beam approach, *Geophys. J. R. astr. Soc.*, **70**, 109–128.

Červený, V., Popov, M. M. & Pšenčík, I., 1982b. Computation of seismic wave fields in laterally inhomogeneous crustal structures – Gaussian beam approach, in *Proc. XVII General Assembly of the European Seismological Commission, Budapest 1980*, pp. 271–275, Akadémiai Kiadó, Budapest.

Červený, V. & Pšenčík, I., 1977. Ray theoretical seismograms for laterally varying layered structures, in *Publ. Inst. Pol. Acad. Sci.*, A-4 (115), pp. 173–185, PWN, Warszawa-Lodz.

Červený, V. & Pšenčík, I., 1979. Ray amplitudes of seismic body waves in laterally inhomogeneous media, *Geophys. J. R. astr. Soc.*, **57**, 97–106.

Červený, V. & Pšenčík, I., 1981. *2-D Seismic Ray Package*, Research Report, Institute of Geophysics, Charles University, Prague.

Červený, V. & Pšenčík, I., 1983. Gaussian beams in two-dimensional elastic inhomogeneous media, *Geophys. J. R. astr. Soc.*, **72**, 419–435.

Červený, V. & Ravindra, R., 1971. *Theory of Seismic Head Waves*, University of Toronto Press.

Chapman, C. H., 1978. A new method for computing synthetic seismograms, *Geophys. J. R. astr. Soc.*, **54**, 481–518.

Chapman, C. H. & Drummond, R., 1983. Body wave seismograms in inhomogeneous media using Maslov asymptotic theory, *Bull. seism. Soc. Am.*, in press.

Claerbout, J. F., 1976. *Fundamentals of Geophysical Data Processing*, McGraw-Hill, New York.

Claerbout, J. F., 1981a. The simplest Gaussian beam, in *Stanford Exploration Project, Rep. No. 28*, pp. 93–97, Department of Geophysics, Stanford University.

Claerbout, J. F., 1981b. The Gaussian beam in energy variables, in *Stanford Exploration Project, Rep. No. 28*, pp. 99–102, Department of Geophysics, Stanford University.

Daley, P. F. & Hron, F., 1982. Ray-reflectivity method for *SH*-waves in stacks of thin and thick layers, *Geophys. J. R. astr. Soc.*, **69**, 527–535.

Deschampes, G. A., 1971. The Gaussian beams as a bundle of complex rays, *Electr. Lett.*, **7**, 684–685.

Felsen, L. B., 1976. Complex-source-point solutions of the field equations and their relation to the propagation and scattering of Gaussian beams, *Inst. Naz. Alta Matem, Symp. Math.*, **18**, 39–56.

Felsen, L. B. & Marcuvitz, N., 1973. *Radiation and Scattering of Waves*, Prentice Hall, Englewood Cliffs.

Fock, V. A., 1965. *Electromagnetic Diffraction and Propagation Problems*, Pergamon Press, New York.

Frazer, L. N. & Phinney, R. A., 1980. The theory of finite frequency body wave synthetic seismograms in inhomogeneous elastic media, *Geophys. J. R. astr. Soc.*, **63**, 691–713.

Fuchs, K., 1968. The reflection of spherical waves from transition zones with arbitrary depth-dependent moduli and density, *J. Phys. Earth*, **16**, 27–41.

Fuchs, K. & Müller, G., 1971. Computation of synthetic seismograms with the reflectivity method and comparison with observations, *Geophys. J. R. astr. Soc.*, **23**, 417–433.

Gabor, D., 1946. Theory of communications, *J. I.E.E.E.*, **93**, 429–441.

Gol'din, S. V., 1979. *Interpretation of Seismic Data Obtained by the Method of Reflected Waves*, Nedra, Moscow (in Russian).

Haddon, R. A. W. & Buchen, P. W., 1981. Use of Kirchoff's formula for body wave calculations in the Earth, *Geophys. J. R. astr. Soc.*, **67**, 587–598.

Hilterman, F. J., 1970. Three-dimensional seismic modelling, *Geophysics*, **35**, 1020–1037.

Hilterman, F. J., 1975. Amplitudes of seismic waves – a quick look, *Geophysics*, **40**, 745–762.

Hong, T. L. & Helmberger, D. V., 1977. Glorified optics and wave propagation in non-planar structures, *Bull. seism. Soc. Am.*, **68**, 1313–1330.

Hron, F., Daley, P. F. & Marks, L. W., 1977. Numerical modelling of seismic body waves in oil exploration and crustal seismology, in *Computing Methods in Geophysical Mechanics*, pp. 21–42, American Society of Mechanical Engineers, New York.

Hron, F. & Kanasewich, E. R., 1971. Synthetic seismograms for deep seismic sounding studies using asymptotic ray theory, *Bull. seism. Soc. Am.*, **61**, 1169–1200.

Hronová, J., 1982. Computation of wave fields in simple structures by the method of Gaussian beams, *diploma thesis*, Charles University, Faculty of Mathematics and Physics, Prague (in Czech).

Hubral, P., 1979. A wave front curvature approach to the computing of ray amplitudes in inhomogeneous media with curved interfaces, *Studia geophys. geod.*, **23**, 131–137.

Hubral, P., 1980. Wave front curvatures in 3-D laterally inhomogeneous media with curved interfaces, *Geophysics*, **45**, 905–913.

Hubral, P. & Krey, Th., 1980. *Interval Velocities from Seismic Reflection Time Measurements*, SEG Monograph Series No. 3, Tulsa.

Hudson, J. A., 1980. A parabolic approximation for elastic waves, *Wave Motion*, **2**, 207–214.

Katchalov, A. P. & Popov, M. M., 1981. The application of the Gaussian beams summation method to the computation of wave fields in the high-frequency approximation, *Dokl. Akad. Nauk. SSSR*, **258** (5), 1097–1100 (in Russian).

Kirpichnikova, N. J., 1971. Construction of solutions concentrated close to rays for the equations of elasticity theory in an inhomogeneous isotropic space, in *Mathematical Problems of Theory of*

Diffraction and Propagation of Waves, Vol. 1, pp. 103–113, Nauka, Leningrad (in Russian, English Translation by American Mathematical Society 1974).

Klem-Musatov, K. D., 1980. *The Theory of Edge Waves and its Applications in Seismology,* Nauka, Novosibirsk (in Russian).

Klimeš, L., 1982a. Mathematical modelling of seismic wave fields in 3-D laterally inhomogeneous media, *Res. Rep. No. 63,* Institute of Geophysics, Charles University, Prague (in Czech).

Klimeš, L., 1982b. Mathematical modelling of seismic wave fields in three-dimensional inhomogeneous media by the expansion into Gaussian beams, *diploma thesis,* Charles University, Faculty of Mathematics and Physics, Prague (in Czech).

Kogelnik, H., 1965. On the propagation of Gaussian beams through lenslike media including those with a loss or gain variation, *Appl. Opt.,* **4,** 1563–1569.

Kravcov, Y. A. & Orlov, Y. I., 1980. *Geometrical Optics of Inhomogeneous Media,* Nauka, Moscow (in Russian).

Landers, T. & Claerbout, J. F., 1972. Numerical calculation of elastic waves in laterally inhomogeneous media, *J. geophys. Res.,* 77, 1476–1482.

Leontovich, M. A. & Fock, V. A., 1946. Solution of the problem of propagation of electromagnetic waves along the Earth's surface using parabolic equation method, *ZETF,* **16,** 557–573 (in Russian).

Marcuse, D., 1972. *Light Transmission Optics,* Van Nostrand, New York.

Maslov, V. P., 1965. *Theory of Perturbations and Asymptotic Methods,* MGU, Moscow (in Russian).

Maslov, V. P., 1977. *Complex Method WKB in Non-Linear Equations,* Nauka, Moscow (in Russian).

May, B. T. & Hron, F., 1978. Synthetic seismic sections of typical petroleum traps, *Geophysics,* **43,** 1119–1147.

McCoy, J. J., 1977. A parabolic theory of stress wave propagation through inhomogeneous linearly elastic solids, *J. appl. Mech.,* **44,** 462–482.

McMechan, G. A. & Mooney, W. D., 1980. Asymptotic ray theory and synthetic seismograms for laterally varying structures. Theory and applications to the Imperial Valley, California, *Bull. seism. Soc. Am.,* **70,** 2021–2035.

Morlet, J. P., 1981. Sampling theory and wave propagation, presented at the *51st Annual Meeting of the SEG,* October 11–15, 1981, Los Angeles.

Morlet, J., Arens, G., Fourgeau, E. & Giard, D., 1982. Wave propagation and sampling theory. Part I: complex signal and scattering in multilayered media, *Geophysics,* **47,** 203–221. Part II: sampling theory and complex waves, **47,** 221–236.

Popov, M. M., 1977. On a method of computation of geometrical spreading in inhomogeneous medium containing interfaces, *Dokl. Akad. Nauk SSSR,* **237,** 1059–1062 (in Russian).

Popov, M. M., 1981. A new method of computations of wave fields in the high-frequency approximation, *preprint LOMI AN SSSR, E-I-81,* Leningrad.

Popov, M. M., 1982. Method of summations of Gaussian beams in isotropic theory of elasticity, *preprint LOMI AN SSSR, P-3-82,* Leningrad (in Russian).

Popov, M. M. & Pšenčík, I., 1978a. Ray amplitudes in inhomogeneous media with curved interfaces, *Geofys. Sb.,* Vol. 24, pp. 118–129, Academia, Praha.

Popov, M. M. & Pšenčík, I., 1978b. Computation of ray amplitudes in inhomogeneous media with curved interfaces, *Studia geophys. geod.,* **22,** 248–258.

Popov, M. M., Pšenčík, I. & Červený, V., 1980. Uniform ray asymptotics for seismic wave fields in laterally inhomogeneous media (abstract), *Prog. Abstr. XVII General Assembly of the European Seismological Commission, Budapest 1980,* p. 143, Hungarian Geophysical Society.

Pšenčík, I., 1979. Ray amplitudes of compressional shear and converted body waves in three-dimensional laterally inhomogeneous media with curved interfaces, *J. Geophys.,* **45,** 381–390.

Pšenčík, I., 1983. Program for the computation of kinematic and dynamic parameters of seismic body waves in 2-D laterally inhomogeneous media with curved interfaces, in *Programs for the Interpretation of Seismic Observations, Vol. 3,* Nauka, Leningrad (in Russian) in press.

Ratnikova, L. I., 1973. *Methods of the Computation of Seismic Waves in Thin-Layered Media,* Nauka, Moscow (in Russian).

Richards, P., 1979. Theoretical seismic wave propagation, *Rev. Geophys. Space Phys.,* **17,** 312–327.

Sinton, J. B. & Frazer, L. N., 1981. Using Kirchhoff's method to compute finite-frequency body wave synthetic seismograms in laterally varying media, *Trans. Am. geophys. Un.,* **62,** 956.

Sinton, J. B. & Frazer, L. N., 1982. A method for the computation of finite frequency body wave synthetic seismograms in laterally varying media, *Geophys. J. R. astr. Soc.,* **71,** 37–55.

Stavroudis, O. N., 1972. *The Optics of Rays, Wavefronts, and Caustics,* Academic Press, New York.

Tappert, F. D., 1977. The parabolic approximations method, in *Wave Propagation in Underwater Acoustics, Lecture Note in Physics,* **70,** 224–287, Springer-Verlag, Berlin.
Trorey, A. W., 1970. A simple theory of seismic diffraction, *Geophysics,* **35,** 762–784.
Trorey, A. W., 1977. Diffraction for arbitrary source-receiver locations, *Geophysics,* **42,** 1177–1182.
Wiggins, R. A., 1976. Body wave amplitude calculations – II, *Geophys. J. R. astr. Soc.,* **46,** 1–10.